การวินิจฉัยสภาพฉนวนของเครื่องจักรกลหมุนโดยใช้การวิเคราะห์ผลตอบสนองไดอิเล็กทริก

INSULATION CONDITION DIAGNOSIS OF ROTATING MACHINE USING DIELECTRIC RESPONSE ANALYSIS

ศิวกร จีนเมือง

SIWAKORN JEENMUANG

วิทยานิพนธ์นี้เป็นส่วนหนึ่งของการศึกษาตามหลักสูตรปริญญาวิศวกรรมศาสตรมหาบัณฑิต

สาขาวิชาวิศวกรรมไฟฟ้าและคอมพิวเตอร์ (หลักสูตรสหวิทยาการ)

คณะวิศวกรรมศาสตร์

สถาบันเทคโนโลยีพระจอมเกล้าเจ้าคุณทหารลาดกระบัง

พ.ศ.2566

KMITL-2023-EN-M-027-073

INSULATION CONDITION DIAGNOSIS OF ROTATING MACHINE USING DIELECTRIC RESPONSE ANALYSIS

SIWAKORN JEENMUANG

A THESIS SUBMITTED IN PARTIAL FULFILLMENT

OF THE REQUIREMENT FOR THE DEGREE OF

MASTER OF ENGINEERING IN ELECTRICAL AND COMPUTER ENGINEERING

(MULTI-DISCIPLINARY PROGRAM)

SCHOOL OF ENGINEERING

KING MONGKUT'S INSTITUTE OF TECHNOLOGY LADKRABANG

2023

KMITL-2023-EN-M-027-073

หัวข้อวิทยานิพนธ์	การวินิจฉัยสภาพฉนวนของเครื่องจักรกลหมุนโดยใช้การวิเคราะห์ผลตอบสนองไดอิเล็กทริก
นักศึกษา	นายศิวกร จีนเมือง
รหัสประจำตัว	64601140
ปริญญา	วิศวกรรมศาสตรมหาบัณฑิต
สาขาวิชา	วิศวกรรมไฟฟ้าและคอมพิวเตอร์ (หลักสูตรสหวิทยาการ)
พ.ศ.	2566
อาจารย์ที่ปรึกษาวิทยานิพนธ์	รศ.ดร.นรเศรษฐ พัฒนเดช
	รศ.ดร. พิทยา ปานนิล

บทคัดย่อ

วิทยานิพนธ์ฉบับนี้นำเสนอการศึกษาสภาพของฉนวนสเตเตอร์ในเครื่องจักรกลหมุน โดยทั่วไปเครื่องจักรกลหมุนจะเผชิญกับความเครียดต่างๆ อย่างต่อเนื่องหลังจากเริ่มต้นใช้งานซึ่งทำให้คุณสมบัติต่าง ๆ ของไดอิเล็กทริกในระบบฉนวนเริ่มกระบวนการเสื่อมสภาพ วิทยานิพนธ์ฉบับนี้นำเสนอการใช้เทคนิคการวัดผลตอบสนองไดอิเล็กทริกเพื่อที่จะนำไปประเมินความสมบูรณ์ของระบบฉนวนของขดลวดสเตเตอร์ โดยการวัดกระโพลาไรเซชันและดีโพลาไรเซชัน และการวัดผลตอบสนองไดอิเล็กทริกในโดเมนความถี่ซึ่งอยู่บนพื้นฐานของการวัดผลตอบสนองไดอิเล็กทริกจะถูกนำไปประยุกต์ใช้งานเพื่อสามารถที่จะวิเคราะห์ความสมบูรณ์ของระบบฉนวนของขดลวดสเตเตอร์ทั้งในโดเมนเวลาและโดเมนความถี่ ตามลำดับ การวัดผลตอบสนองไดอิเล็กทริกในเครื่องกำเนิดไฟฟ้าและมอเตอร์ 5 กรณีศึกษา ในกรณีของเครื่องกำเนิดไฟฟ้าได้นำเสนอการศึกษาเชิงเปรียบเทียบระหว่างเครื่องกำเนิดไฟฟ้าที่พิกัดและประเภทเดียวกัน ในกรณีของมอเตอร์ ได้นำเสนอกรณีศึกษาต่าง ๆ ซึ่งเกี่ยวข้องกับผลกระทบของสิ่งปนเปื้อน ผลของการทำความสะอาดและอบไล่ความชื้น มอเตอร์ที่ตรวจพบระดับของการดิสชาร์จบางส่วนที่สูง ซึ่งดำเนินการทดสอบระหว่างการบำรุงรักษา จากผลการทดสอบพบว่า การวัดผลตอบสนองไดอิเล็กทริกเป็นเครื่องมือที่มีประสิทธิผลซึ่งสามารถประเมินความสมบูรณ์ของฉนวนขดลวดสเตเตอร์ได้ทั้งในสภาพพื้นผิวและภายในเนื้อฉนวนได้

Thesis	INSULATION CONDITION DIAGNOSIS OF ROTATING MACHINE USING DIELECTRIC RESPONSE ANALYSIS
Student	Mr. Siwakorn Jeenmuang
Student ID.	64601140
Degree	Master of Engineering
Program	Electrical and Computer Engineering (Multi-Disciplinary Program)
Year	2023
Thesis Advisor	Assoc. Prof. Dr. Norasage Pattanadech Assoc. Prof. Dr. Pittaya Pannil

ABSTRACT

This thesis presents an investigation of the stator winding insulation condition of rotating machines. Typically, such machines continuously encounter various stresses once they are in service, which causes to degrade of the dielectric properties of the insulation system. The dielectric response measurement (DRM) was utilized in this research to evaluate the integrity of the stator winding insulation system. Polarization and depolarization current (PDC) and frequency domain spectroscopy (FDS), as techniques based on DRM, were employed to allow such analysis in both time and frequency domains, respectively. 5 case studies of the application of DRM on generators and motors are presented. In the case of generators, the comparison between two generators with the same rate and type using PDC is presented and discussed. In the case of motors, case studies associated with the effect of contamination, the cleaning and drying process of motors, and a motor with high levels of partial discharge, during maintenance are presented and discussed. The test results show that the DRM is an effective task that can evaluate the integrity of the stator winding insulation in both surface and bulk conditions.

Acknowledgement

First of all, I would like to express my sincere gratitude to my supervisor, Assoc. Prof. Dr. Norasage Pattanadech for his professional advice and encouragement to deeply study high voltage engineering and for providing the opportunity valuable experience. I sincerely appreciate all of your valuable comments, advice, corrections, and endless support. Moreover, I would like to express my gratitude to Assoc. Prof. Dr. Pittaya Pannil for serving as the second supervisor.

I would like to acknowledge Mr. Tanet Wor-thong who provided the opportunity for gaining invaluable knowledge and experience in the power plant.

Special thanks are also given to Mr. Suriya Mongkolsatitpong, PD Solutions Co., Ltd., and Plan Market Gold Co., Ltd. for his kind support of the PD instrument, and for sharing his invaluable experience.

Special thanks are also given to Mr. Worachai Sawatdimongkol, TIS Engineering and Service CO., LTD. for his kind support of Omicron DIRANA for performing the experiment in this work.

Special thanks are also given to Mr. Suwapich Likitsupin and Mr. Suthat Suksagoolpanya for their guidance about the high voltage testing.

Special thanks are also given to Dr. Somyot Tantipattarakul for teaching deep knowledge of polymer theory and dielectric response measurement.

I would like to acknowledge all seniors in Dielectric Analytika and High Voltage Engineering Laboratory (Dika Lab), Dr. Sakda Maneerot, Dr. Phetai Nimsanong, Asst. Prof. Kittisak Thungsook, Mr. Kittipod Jariyanurat, Miss Natnaree Phumipunepon, Mr. Chaitawat Chuayin, Miss Korraya Jongvilaikasem, Mr. Yannaphol Kittikhuntharadol for his/her guidance and sharing their experiences, and also continuous supports. Mr. Kritsada Dorkmai, Mr. Patt Udomluksananon, Mr. Komin Chumpiboon, Mr. Warisanan Rojanasunan, and so on for providing a great work atmosphere and teamwork.

Last but not least, I want to convey my sincere gratitude to my family, especially my dear parents, for their love, greatest motivation, and unwavering support during this project. Without their love, passion, and patience, this effort would not have been possible. To my beloved Ranchana, who always supported me and stood by me when I felt discouraged. I sincerely thank you and love you.

Siwakorn Jeenmuang

Contents

LIST OF TABLES

Page

LIST OF FIGURES

Page

Chapter 1
Introduction

1.1 Statement and significance of the problems

Rotating machines play an important role in the power system in several sections. Generator is an important asset that is utilized to generate electrical power into a power grid. In addition, motors are also an important asset that is used in vast industries, for instance, pumps, conveyors, and so on. Hence, the premature failure of such a machine has to be avoided because it can force an outage and lead to a loss amount of cost. The reliability of such equipment depends mainly on the insulation as stator winding insulation is one of the most vulnerable parts subjected to several stresses during service. Such stresses i.e., TEAM stress can deteriorate the stator winding insulation which leads to the alteration of material properties (aka degradation). Therefore, to ensure the reliability and safe operation of such equipment, effective methods for evaluating the stator winding insulation condition are needed to prevent unexpected failure of rotating machine e.g., Partial discharge (PD), Dielectric dissipation factor ($\tan\delta$), and also Dielectric response measurement (DRM).

PD measurement is one of the most effective methods to evaluate the "local" insulation condition of high-voltage apparatus, especially rotating machines. Once the insulation system has deteriorated, it can lead to PD taking place. Any failure process that generates PD as a symptom of insulation aging and/or degradation can be detected with this method [1].

For evaluating "integral" insulation conditions, several methods are used. Traditionally, insulation resistance (IR) and polarization index (PI) has been used for a long time as basic tool which is done by megaohm-meter. Besides, performing the dielectric dissipation factor (or power factor) at power frequency (50/60 Hz) has also been used as well as power factor tip-up has also been used as an indirect way to determine the PD inception voltage (PDIV) in the past. However, single or two values from IR and PI and also $\tan\delta$ are usually not sufficient to determine the insulation problems. The better way is to perform the current measurement overtime to plot the polarization and depolarization current (PDC) in case of the time domain

measurement and to measure $\tan\delta$ over a wide range of frequency i.e., frequency domain spectroscopy (FDS). These methods successfully evaluated the insulation condition of the power transformer and power cable. However, in the case of rotating machines, more investigations are still needed to completely define the evaluation criteria.

1.2 Goal and objective

- To study the stator winding insulation systems of rotating machine
- To understand the degradation processes and failure mechanisms of the stator winding insulation of rotating machine
- To study the application of dielectric response measurement in both time and frequency domains on the insulation system of high voltage equipment, especially rotating machine
- To evaluate the stator winding insulation condition of rotating machine using dielectric response measurement

1.3 Scope

This thesis covers the application of dielectric response measurement in both time and frequency domains on the stator winding insulation of rotating machine either generator or motor as an effective method to evaluate the stator winding insulation condition.

1.4 Hypothesis

The stator winding insulation of rotating machine is degraded with time over its service life depending on various stresses that the stator winding insulation is subjected to. A dielectric response measurement (DRM) is a tool that has the ability to evaluate the integral condition of the stator winding insulation.

1.5 Process of the study

Table 1.1 Process of the study

Operation	Semester 1, Academic Year 2021					Semester 2, Academic Year 2021				
	Aug	Sep	Oct	Nov	Dec	Jan	Feb	Mar	Apr	May
1. Study the theory of stator winding insulation of rotating machine										
2. Study the theory of dielectric response measurement										
3. Experiment in the laboratory										
4. On-site investigation										
5. Analyze the test results										
Operation	**Semester 1, Academic Year 2022**					**Semester 2, Academic Year 2022**				
	Aug	Sep	Oct	Nov	Dec	Jan	Feb	Mar	Apr	May
4.On-site measurement										
5. Analyze the test results										
6.Conference participation (CMD2022, Kitakyushu, Japan)										
7.Thesis preparation										

Chapter 2

Theory

This chapter describes the basic knowledge of rotating machine structures. Basic theory and overviews of dielectric response measurement in either time or frequency domain including its application, are provided in this chapter.

2.1 Stator winding insulation

2.1.1 Type of stator winding construction

There are three types of stator winding construction that are generally used with a vast range of power ratings, from a few kW for small machines up to several GW for very large generators [1]:

- Random-wound stators
- Form-wound stators: multi-turn coils of stator coils
- Form-wound stators: Roebel bars or stator bars

However, this thesis only intended to consider the form-wound stators which are typically applied for high voltage applications [1-3].

2.1.1.1 Random-wound stators

This type of stator windings is typically used in low-voltage machines with relatively low power ratings. They consist of round-shaped thinly insulated copper conductors that are wound together in the slots in the stator core to produce a coil, as shown in Fig. 2.1. This type of stator winding is not taken into account in this thesis.

Fig. 2.1 Random-wound stator.

2.1.1.2 Form-wound: stator coils

Form-wound stators are usually found in rotating machines operated at 1 kV and above. This type of stator winding is made from the insulated coil to form the coil to be a so-called “Diamond shape”. The strand conductors usually have a rounded-rectangular-shape. This type of stator winding covers most motors and medium range of generators [1]. The form-wound stator coils and complete winding are illustrated in Fig. 2.2.

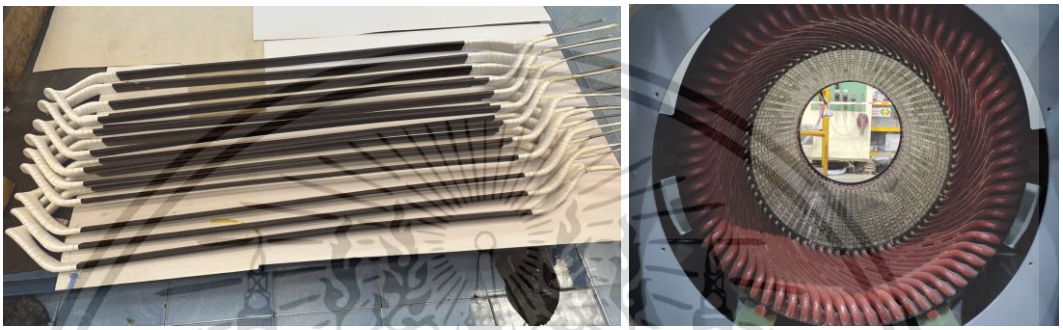

(a) (b)

Fig. 2.2 Form-wound (a) stator coils and (b) complete winding.

2.1.1.3 Form-wound: roebel bar

This type of stator winding is usually found in large generators i.e., at a power rating above 50 MVA. Since the form-wound coil is large, it may be difficulties to insert both legs of the coil in the slot without risking mechanical damage. Thus, most large generators today are not made from multi-turn coils, but rather from “half-turn” coils, often referred to as Roebel bars. With the Roebel bar approach electrical connections to make the “coils” are needed at both ends of the bar [1]. The form-wound stator bars and complete winding are illustrated in Fig. 2.3.

(a) (b)

Fig. 2.3 Form-wound (a) stator bars and (b) complete winding.

2.1.2 Stator winding insulation systems

The stator winding insulation systems are comprised of several components. The components of the stator winding insulation systems in the slot portion are illustrated in Fig. 2.4.

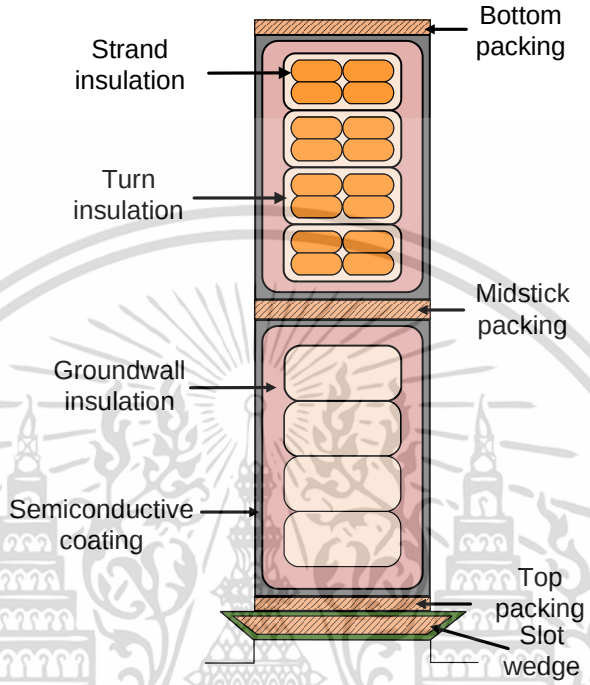

Fig. 2.4 Components of the stator winding insulation systems in the slot portion [1].

The actual cross-section of the stator winding in the slot portion is illustrated in Fig. 2.5.

Fig. 2.5 Cross-section of the stator coils in the slot portion.

2.1.2.1 Strand insulation

The individual strand conductors are usually insulated. Strand insulation can be made up of organic resin enamels, polymeric films, resin-bonded fibers (such as

paper, cotton, asbestos, glass, polyester, or combinations of them) or resin-bonded mica [3].

2.1.2.2 Turn insulation

In a coil with more than one turn, groups of strands forming a single turn (conductor) may be held together and insulated [3].

2.1.2.3 Groundwall insulation

Groundwall insulation is the component that separates the copper conductors from the grounded stator core. Failure of groundwall insulation can lead to ground fault and forced outage of the motor or generator. Thus, the stator groundwall insulation is critical to the proper operation of a motor or generator. For a long service life, the groundwall must meet the rigors of the electrical, thermal, and mechanical stresses that it is subject to [1]. In the electrical aspect, the groundwall insulation should have high electrical strength to withstand operating phase-to-ground voltage or stress. In the thermal aspect, the groundwall insulation should have a low thermal resistivity to transmit the heat generated from the copper conductors into the stator core [1, 2].

2.1.2.4 Semiconducting slot coating

The surface of slot portions of stator coils and bars, including several centimeters of the coil beyond the core, is normally semiconducting. These treatments are often referred to as conductive and are generally applied to machines with a rated voltage of 4 kV and above [3]. To prevent PD on the coil or bar surfaces, manufacturers have long been coating the coil/bar in the slot area with a partly conductive coating [1]. This coating, often called a semiconductive or Semicon coating, is likely to be in contact with the grounded stator core at many places along the length of the slot.

2.1.2.5 Stress control coating

The semiconductive slot coating with low resistance usually extends only a few centimeters beyond each slot exit.

The small radius of the edge of the semiconductive slot coating is explained by the needle (with the voltage of V) with radius r and distance d between the needle and ground plane, which produce the maximum electrical field stress at the needle tip of approximately [1]:

$$E = \frac{2V}{r \ln\left(\frac{4d}{r}\right)} \tag{2.1}$$

Like underground cable, the electric field enhancement at this sharp edge will lead to discharge which degrades the insulation at that part. Thus, the stress control coating (usually silicon carbide, SiC) is used to grade the electric field in that area uniformly, thus reducing the electrical field concentration. This material is characterized by “non-linear “properties, in which if the electric field is increased, the resistance will decrease. This principle is similar to the application of a high-voltage arrester. The stress control coating was applied over the semiconductive slot coating along the endwinding surface resulting in varying resistance with distance. This varying resistance yields the electric field at the sharp edge of the semiconductive slot coating more uniform. The concepts of applying the stress control coating are depicted in Fig. 2.6.

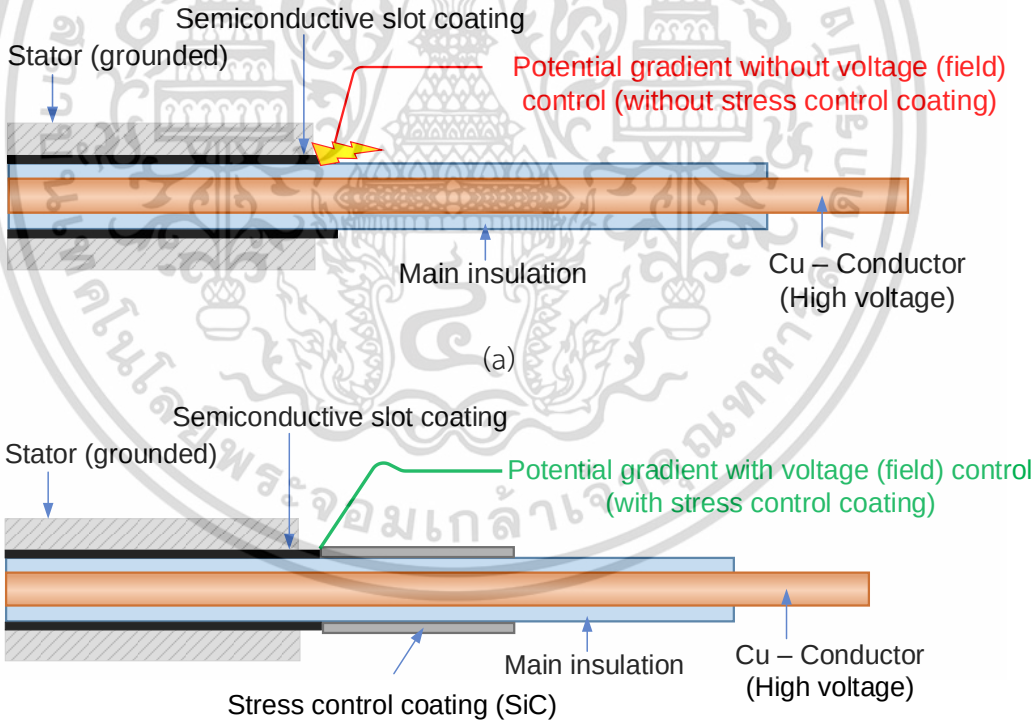

Fig. 2.6 (a) without stress control grading (b) with stress control grading.

The actual insulation system of the overhang or endwinding region is illustrated in Fig. 2.7.

Fig. 2.7 Insulation system in the slot exit area.

2.2 Failure mechanisms of stator winding insulation

The reliability of HV equipment is dependent mainly on the stator winding insulation system, which can be regarded as a weak point part of HV equipment. Thus, it needs to ensure and take care of the insulation to get reliable use in service.

It can briefly explain the failure mechanisms of the stator winding insulation. Practically, in operation, the insulation of the generator can encounter various stresses, i.e., Thermal, Electrical, Ambient (or Atmosphere), and Mechanical, also known as TEAM stresses, resulting in insulation degradation [1]. Such stresses are mainly presented simultaneously as combined stress which accelerates the aging of the stator winding insulation.

There are several failure mechanisms of the stator winding insulation system that will lead to machine failures. For this reason, this section focuses mainly on the degradation and deterioration process of machine insulation in service life as follows [1]:

- Thermal deterioration
- Thermal cycling
- Contamination (Electrical tracking)
- Loose coils in the slot
- Vibration sparking
- Endwinding vibration
- Etc.

2.3 Dielectric response

2.3.1 Basic theory

Theoretically, the fundamental principle of dielectric properties can be explained by determining the vacuum dielectric with electrode arrangement. The relationship between "dielectric flux density" D which is proportional to the applied electric field E with a time-varying function [4-7].

$$D(t) = \varepsilon_0 E(t) \tag{2.2}$$

where ε_0 =8.85419 × 10^{-12} As/Vm is the permittivity of free space or vacuum.

If a particular vacuum dielectric is replaced by some kind of dielectric material with the same electrode arrangement. The term "polarization" P is added in the equation (2.2), resulting in

$$D(t) = \varepsilon_0 E(t) + P(t) \tag{2.3}$$

The term "polarization" P depends on the different polarization process mechanisms after exciting the "electric field" E into the dielectric material. When the step voltage (or electric field) is excited at the time $t = 0$, the dielectric material will be characterized by the "susceptibility" $\chi(t)$ as the response in the time domain as illustrated in Fig. 2.8.

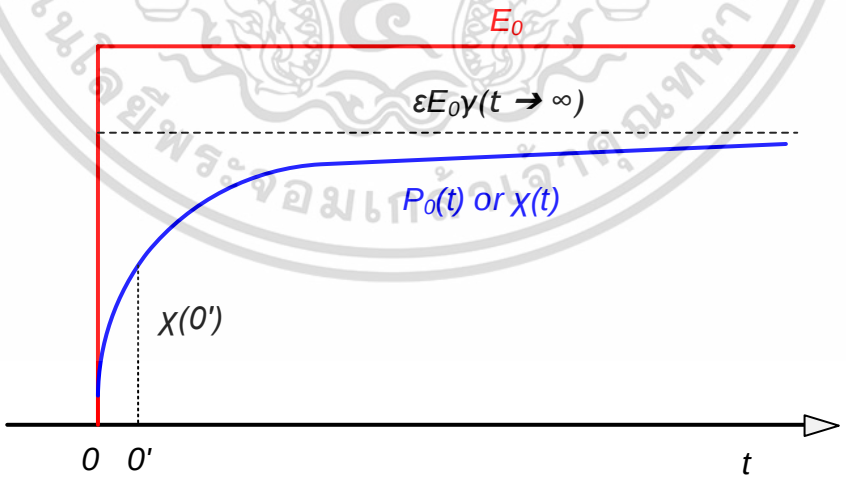

Fig. 2.8 Polarization of a dielectric material subjected to an electrical step field of magnitude $E(t) = E_0$ [5].

For an arbitrary time-dependent electrical field $E(t)$, then the polarization $P(t)$ can be obtained.

$$P(t) = \varepsilon_0 \chi E(t) + \Delta P(t) = \varepsilon_0 \chi E(t) + \varepsilon_0 \int_0^t f(\tau) E(t-\tau) d\tau \tag{2.4}$$

where $f(t)$ is the dielectric response function.

$$f(t) = \frac{d\chi(t)}{dt} \tag{2.5}$$

Regarding the maxwell equations, it can be expressed in terms of "current density, $j(t)$" which is expressed by the summation of conduction and displacement current components.

$$j(t) = \sigma_0 E(t) + \frac{dD(t)}{dt} \tag{2.6}$$

where σ_0 is DC conductivity

From equation (2.3), substitute the "dielectric flux density" $D(t)$ in equation (2.6)

$$j(t) = \sigma_0 E(t) + \varepsilon_0 \frac{dE(t)}{dt} + \frac{dP(t)}{dt} \tag{2.7}$$

And also, substitute the polarization $P(t)$ in equation (2.7)

$$j(t) = \sigma_0 E(t) + \varepsilon_0 \frac{d}{dt}\left\{ \varepsilon_r E(t) + \int_0^t f(\tau) E(t-\tau) d\tau \right\} \tag{2.8}$$

where ε_r is the relative permittivity of dielectric material.

From equation (2.8), it can be re-written in terms of "current, $i(t)$" instead of "current density, $j(t)$". In the same way, the excitation electric field $E(t)$ is replaced by applied voltage $u(t)$, which is simplicity to be used and explained in practical terms.

$$i(t) = C_0 \left[\frac{\sigma_0}{\varepsilon_0} u(t) + \varepsilon_\infty \frac{du(t)}{dt} + \frac{d}{dt} \int_0^t f(t-\tau) u(\tau) dt \right] \tag{2.9}$$

where C_0 is the geometric of vacuum capacitance of the test object. ε_∞ is the high-frequency component of permittivity.

From equation (2.9), this is the general equation of the dielectric response in the time domain of dielectric material where input is voltage excitation and output are the current response that flows through the dielectric material.

From equation (2.9), determine the voltage step excitation as a "step DC voltage" excitation at the time $t=0$ with $u(t)=U_c$.

$$u(t)=\begin{Bmatrix} 0,\ t<0 \\ U_c,\ 0\le t\le t_c \\ 0,\ t>t_c \end{Bmatrix} \tag{2.10}$$

Therefore, the step response will be characterized by the so-called "polarization current, $i_{pol}(t)$" as follows.

$$i_{pol}(t)=C_0U_c\left[\frac{\sigma_0}{\varepsilon_0}+\varepsilon_\infty\delta(t)+f(t)\right] \tag{2.11}$$

where $\delta(t)$ is the Dirac function.

If neglecting the second term in equation (2.11) since it takes place at very short time and is impossible to be measured in practical, which can be re-written as follows.

$$i_{pol}(t)=C_0U_c\left[\frac{\sigma_0}{\varepsilon_0}+f(t)\right] \tag{2.12}$$

Thereafter, once the dielectric material was charged with charging time of t_c i.e., the time duration during applying the step DC voltage excitation. Then, the excitation voltage was disconnected, and the dielectric material was shorted circuit. The current response measured will be discharged with an opposite directional current of polarization current and will be characterized by the so-called "depolarization current, $i_{dep}(t)$" as follows.

$$i_{dep}(t)=-C_0U_c\left[\varepsilon_\infty\delta(t)+f(t)-f(t+t_c)\right] \tag{2.13}$$

As addressed above we can also neglect the first term in equation (2.13), which can be re-written as follows.

$$i_{dep}(t)=-C_0U_c\left[f(t)-f(t+t_c)\right] \tag{2.14}$$

The principle of step response with step excitation magnitude of U_c and charging time is illustrated in Fig. 2.9.

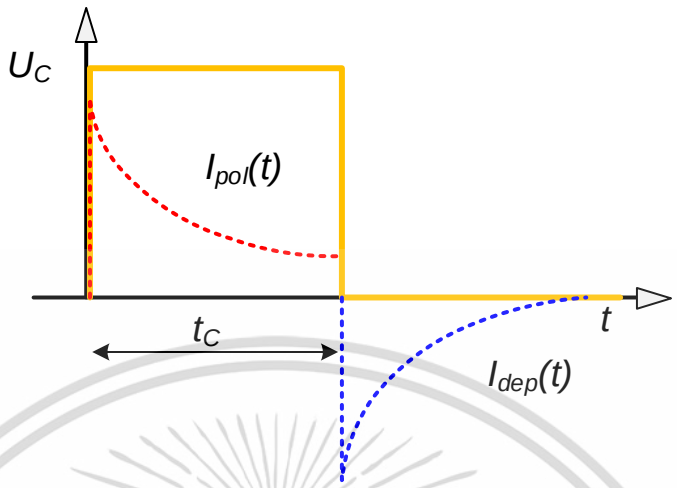

Fig. 2.9 Principle of relaxation current measurement [8].

From equation (2.14), it was found that if the dielectric material was charged for a sufficiently long time, $f(t+t_c) \simeq 0$, the depolarization current will be regarded as a "complete dielectric response" and can be re-written as

$$i_{dep}(t) \approx -C_0 U_c f(t) \tag{2.15}$$

Therefore, it was found that the dielectric response function $f(t)$ is proportional to the depolarization current, $i_{dep}(t)$ and can be estimated.

$$f(t) \approx -\frac{i_{dep}(t)}{C_0 U_c} \tag{2.16}$$

Besides, if the dielectric material was charged for a sufficiently long time, $f(t+t_c) \simeq 0$, the conductivity will be estimated by summation of the polarization current $i_{pol}(t)$ and depolarization current $i_{dep}(t)$ as follows.

$$\sigma_0 \approx \frac{\varepsilon_0}{C_0 U_c}\left(i_{pol}(t) - i_{dep}(t)\right) \tag{2.17}$$

Both dielectric response function $f(t)$ and conductivity, σ_0 are of importance parameters to characterize the dielectric material in both polarization and conduction phenomena in the dielectric material, respectively. However, these parameters will be based on simplified dielectric material with knowing dimensions and homogeneous insulation. In contrast, it is impossible to obtain the following parameters since realistic

insulation systems of high voltage equipment are complex and usually composite with different kinds of material.

Concerning the frequency domain of the dielectric properties, it can start with the response in the time domain and then be converted into the frequency domain using Laplace or Fourier Transformation. From equation (2.9), using Fourier Transformation can be converted into frequency domain as follows.

$$\hat{I}(\omega) = j\omega C_0 \left[\varepsilon_\infty + \chi'(\omega) - j\left(\frac{\sigma_0}{\varepsilon_0 \omega} + \chi''(\omega) \right) \right] \hat{U}(\omega) \tag{2.18}$$

where

$$\chi(\omega) = \chi'(\omega) - j\chi''(\omega) \tag{2.19}$$

and

$$\varepsilon(\omega) = \varepsilon'(\omega) - j\varepsilon''(\omega) \tag{2.20}$$

The dielectric dissipation or dielectric loss factor $\tan\delta$ can be defined as follows.

$$\tan\delta(\omega) = \frac{\varepsilon''(\omega)}{\varepsilon'(\omega)} = \frac{\frac{\sigma_0}{\varepsilon_0 \omega} + \chi''(\omega)}{\varepsilon_\infty + \chi'(\omega)} \tag{2.21}$$

2.3.2 Polarization mechanisms

The main polarization mechanisms will be explained below [9].

- **Electronic Polarization** (also called optical polarization): The electric field causes deformation or translation of the originally symmetrical distribution of the electron clouds of atoms or molecules. This is essentially the displacement of the outer electron clouds with respect to the inner positive atomic cores.
- **Atomic Polarization** or ionic polarization: The electric field causes the atoms or ions of a polyatomic molecule to be displaced relative to each other. This is essentially the distortion of the normal lattice vibration, and this is why it is sometimes referred to as vibrational polarization.
- **Orientation Polarization**: This polarization occurs only in materials consisting of molecules or particles with a permanent dipole moment.

The electric field causes the reorientation of the dipoles toward the direction of the field.

- **Space charge polarization, or interfacial polarization**, is produced by the separation of mobile positively and negatively charged particles under an applied field, which form positive and negative space charges in the bulk of the material or at the interfaces between different materials.

2.3.3 Dielectric response measurement in the time domain

2.3.3.1 Polarization and Depolarization Current (PDC) measurement

Theoretically, the principle of Polarization and Depolarization Current (PDC) measurement is when applying a step DC voltage across the insulation, while the current flowing through the insulation was measured using an appropriate ampere meter (pico ammeter, or electrometer), which is able to measure the current down to the pico-ampere range up to milli-ampere range [4]. The current measured in which a step DC voltage (U) was applied is the so-called polarization current (or so-called charging current, relaxation current). Thereafter, when the voltage source was then removed and the insulation under test was short-circuited. The current measured in this process is the so-called depolarization current (or discharging current). The principle of test arrangement for PDC measurement is schematically shown in Fig. 2.10.

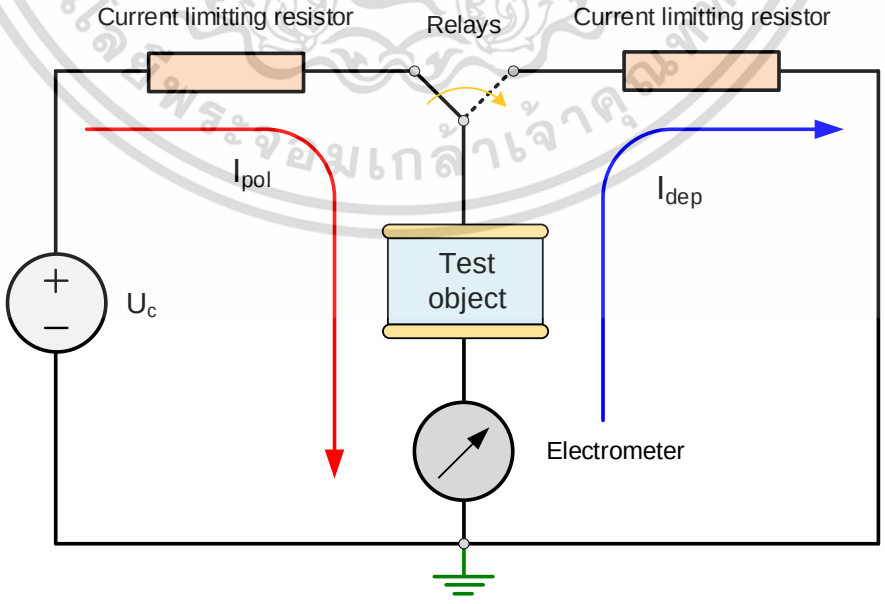

Fig. 2.10 Principle of a test circuit for PDC measurement [10].

The principle of polarization current component is illustrated in Fig. 2.11

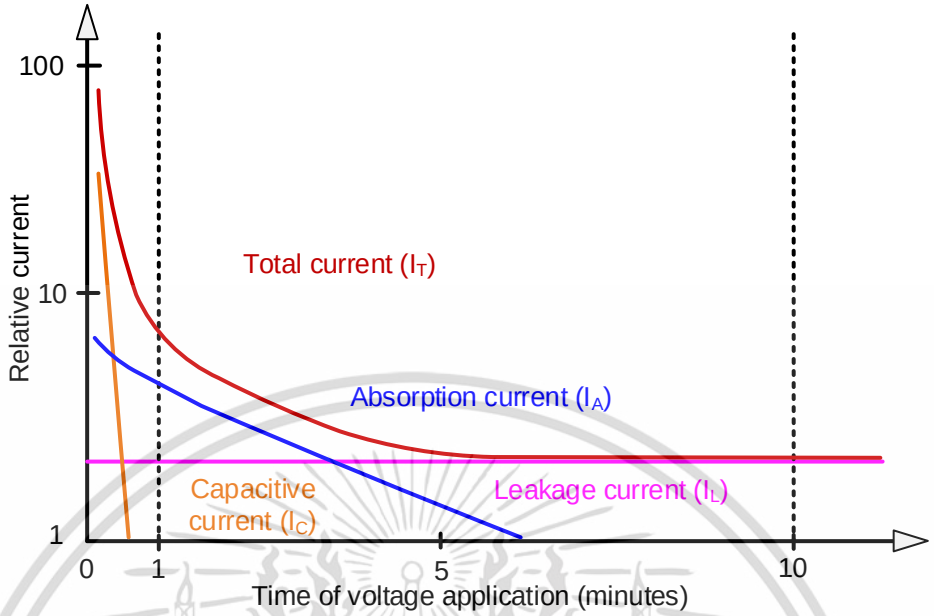

Fig. 2.11 Principle of polarization current [11].

As Fig. 2.11, the total current $i_t(t)$ (refers to polarization current $i_p(t)$) when a step voltage is applied is comprised of mainly 3 components as follows:

- **Capacitive current**, $i_c(t)$: This term is caused by changing of electric field excitation instantaneously ($i_c(t) = C\,du/dt$). This current component occurs in a short time and decays with a time constant, depending on the series resistance of the test circuit and the capacitance of the test object. This current component is not used in insulation diagnostics.
- **Absorption current**, $i_a(t)$: This current component is caused by the polarization processes from dipolar and interfacial polarization. This current decay to nearly zero for a long time depending on the insulation material.
- **Leakage current**, $i_l(t)$: leakage current term occurs when the voltage source is applied to the insulation. This current component could be from leakage current from the surface and bulk currents. This term is related to moisture absorption or conductive contamination over the surface of the insulation system.

The basic parameters extracted from polarization current which is used for a long time using “Megaohm meter” i.e., insulation resistance (IR) and polarization index (PI).

- Insulation resistance (IR)

As defined in IEEE std 43 [11], Insulation resistance (IR) is the capability of the electrical insulation to resist direct current. The quotient of applied direct voltage (usually negative polarity) divided by current across the insulation.

$$IR_{1\min} = \frac{U_c}{i(60s)} \tag{2.21}$$

- Polarization index (PI)

As defined in IEEE std 43 [11], the Polarization index (PI) is a variation in the value of insulation resistance with time. The quotient of the insulation resistance at time (t_2) is divided by the insulation resistance at time (t_1). The times t_2 and t_1 are 10 min and 1 min, respectively.

$$PI = \frac{IR_{10\min}}{IR_{1\min}} \tag{2.22}$$

PDC measurement was used for many decades to evaluate the state of the insulation system of HV apparatus, for instance, power transformers [13], power cables [14], and also rotating machines. In power transformer or some oil-paper insulation system, the PDC measurement can be performed to obtain the moisture content in the cellulose (or paper) insulation and the conductivity of the insulating oil insulation by fitting the test results using X-Y model and comparison with the database [15]. In power cables, PDC measurement could evaluate “water treeing” in the cross-linked polyethylene (XLPE) [16] and also ethylene propylene rubber (EPR) insulation. For rotating machines, the PDC measurement is an effective tool to indicate the contamination of the insulation system as a surface condition and is also able to evaluate the aging and degradation mechanism of the bulk insulation [17-19].

Besides the PDC measurement in the time domain, recovery voltage measurement (RVM) was also used [20]. There was also a tool that was able to evaluate the insulation condition in HV apparatus, especially for power transformers and cables. Furthermore, another alternative analysis, the so-called Isothermal relaxation current (IRC) is also used. This technique was originally mainly used to

investigate PE and XLPE cable insulation [6, 14]. The method is based on the depolarization current measurement which is usually performed by applying a voltage of 1 kV with a charging time of 1800 s (30 min) and then followed by the discharging period. The measured depolarization current is then multiplied by time resulting in the IRC plot [6].

2.3.4 Dielectric response measurement in the frequency domain

Traditionally, the dielectric response in the frequency domain was used for a long time by performing the capacitance and dielectric loss factor (C & $\tan\delta$) measurement at power frequencies (50/60 Hz) [21]. Also, tip-up is an alternative way to evaluate the insulation condition, especially in a rotating machine as it can determine the PD inception voltage (PDIV) level indirectly [21]. However, in many literatures, only a single discrete frequency (50/60 Hz) revealed that may not sufficiently characterize the insulation condition of high-voltage equipment. Therefore, the dielectric response analysis in a wide range of frequencies is of interest.

The basic theory of frequency domain spectroscopy (FDS) is when excitation of the voltage $\hat{U}(\omega)$ with sinusoidal waveform at difference frequencies across the interest insulation system and then measures the current response $\hat{I}(\omega)$ of a particular insulation. The principle of FDS is illustrated in Fig. 2.12.

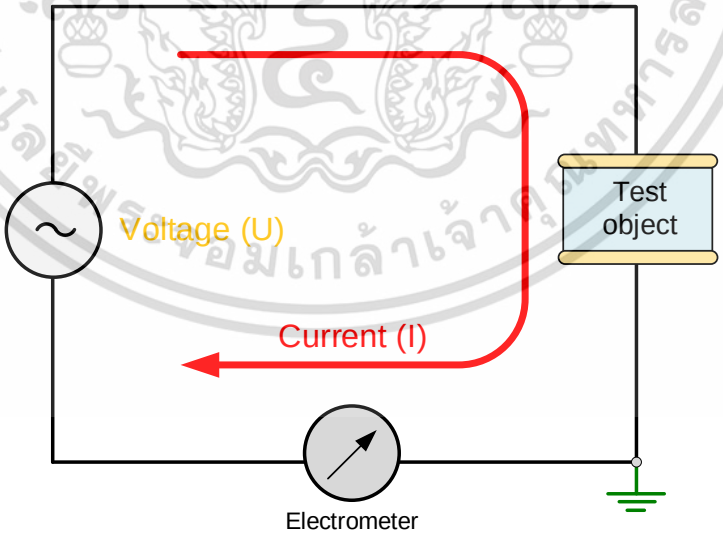

(a)

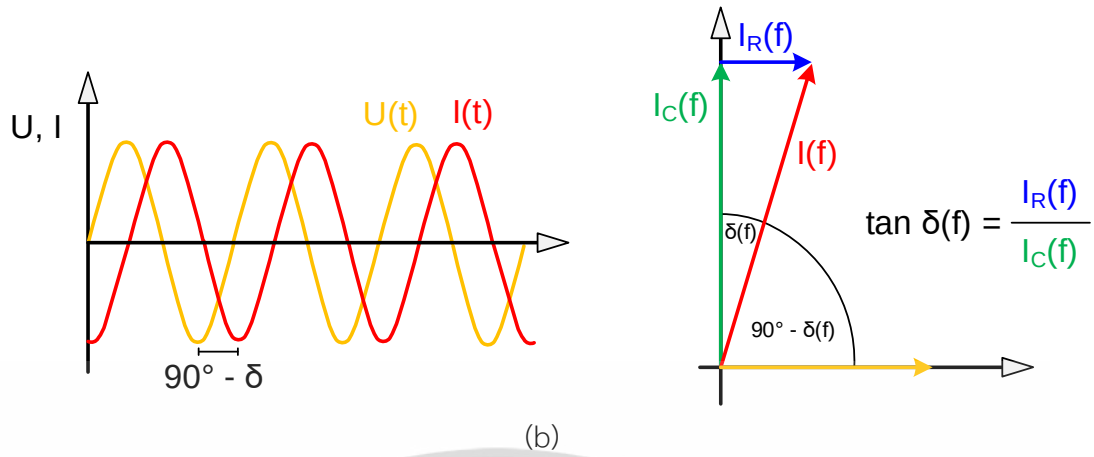

(b)

Fig. 2.12 (a) Principle of a test circuit for FDS (b) phasor diagram of voltage and current [22].

Accordingly, the impedance $Z(\omega)$, complex capacitance $C(\omega)$, and dielectric loss factor $\tan\delta$ can be calculated.

$$\frac{\hat{U}(\omega)}{\hat{I}(\omega)} = Z(\omega) = Z'(\omega) + jZ''(\omega) \tag{2.23}$$

In the high-voltage engineering field, complex capacitance is usually used instead of complex permittivity. So, the impedance can be assumed as complex capacitance $C(\omega)$ in which the quantity can be directly measured by dielectric spectrometer [8], hence in can be defined the relation between voltage excitation $\hat{U}(\omega)$ and measured current $\hat{I}(\omega)$

$$\hat{I}(\omega) = j\omega C(\omega)\hat{U}(\omega) \tag{2.24}$$

where

$$C(\omega) = C'(\omega) - C''(\omega) \tag{2.25}$$

Therefore, the dielectric loss factor $\tan\delta$ can be rewritten using the equation.

$$\tan\delta = \frac{C''(\omega)}{C'(\omega)} \tag{2.26}$$

The FDS is conducted over a wide range of frequencies, typically 1 kHz – 1 mHz or even lower. The test usually starts at a higher frequency and stops at a low frequency to reduce the effect of remnant charged which can be regarded as “memory effect” introduced in a lower frequency range [15, 23].

Like PDC measurement, FDS can be used to evaluate the insulation condition of the HV apparatus. Typically, the FDS is preferred as a tool for power transformer and cable insulation due to its better sensitivity compared with that of the PDC measurement. However, the drawback of FDS is time-consuming since to get more information about the state of insulation, it needs to perform more deep frequency i.e., lower frequency, for instance, IEEE std C57.161 [15] stated that the sufficient frequency to evaluate the insulation of power transformer is about 10 mHz – 0.1 mHz which depends on temperature, insulation dryness, and condition of the oil [15]. Therefore, the lower the stop frequency, the more time-consuming will be. For example, at the point of stop frequency of 0.1 mHz, time consuming is about 2.8 hours, which is inappropriate in practical.

To overcome the drawback of FDS, the combination of both PDC measurement and FDS is proposed [24]. Both advantages of those two techniques are used by performing the FDS at the higher range of frequency typically 1 kHz – 10 mHz, and then performing the PDC measurement to convert the current data into frequency domain (< 10 mHz).

2.4 Application of PDC measurement and FDS for rotating machine

Nowadays, PDC measurement and FDS are often employed as non-destructive test methods to evaluate the insulation condition of the rotating machine. However, up to now, there are still not standardized methods as other HV equipment i.e., power transformers. However, some parts of international standards have stated this method to be used in rotating machines, especially PDC measurement [11, 12]. Moreover, Cigre working groups A1.17 and A1.26 [10, 25] contained the PDC measurement methods to apply for HV motors which were mainly based on the research work of Supatra A. Bhumiwat [19], which can be regarded as she is a pioneer who used the PDC measurement to apply in several HV equipment in Thailand.

Much research is associated with both studies of stator winding insulation by performing the accelerating test in the laboratory to investigate dielectric properties when subjected to several simulating stresses. The aim of this is to make an effort to link the evaluation condition to the real machine in service.

There are several commercial instruments providing the ability to perform PDC and FDS measurements in high-voltage equipment, as an example in Fig. 2.13.

(a) (b)

Fig. 2.13 Commercial dielectric response analyzer (a) PDC analyzer (Alff engineering, Switzerland) (b) PDC&FDS analyzer (Omicron DIRANA, Austria).

Chapter 3

Experimental Details

In this chapter, the experimental details associated with the dielectric response measurement are explained. Several measuring circuit configurations are shown. Things to do before the dielectric response measurement are introduced. Besides, how to analyze the dielectric response measurement results are demonstrated.

3.1 Dielectric response measurement circuits of rotating machine

As mentioned in Chapter 2, the dielectric response measurement can be conducted on the rotating machine in difference measuring configurations depending on the insulation to be investigated. Principally, one should know about the insulation parts of the rotating machine insulation systems. Fig. 3.1 illustrates the typical insulation in different parts which comprise the phase-to-ground insulation and phase-to-phase (interphase) insulation. Phase-to-ground insulation, as simply represented by elements of C_A, C_B, and C_B for the insulation between winding and laminated core of phases A, B, and C, respectively. For phase-to-phase insulation (C_{AB}, C_{BC}, and C_{CA}), there are the insulation parts between phases which are mainly found at the endwinding (overhang region). Since in the slot portion stator coils/bars are shielded as ground potential by semiconductive coating, the phase-to-phase insulations in the slot portion never exist.

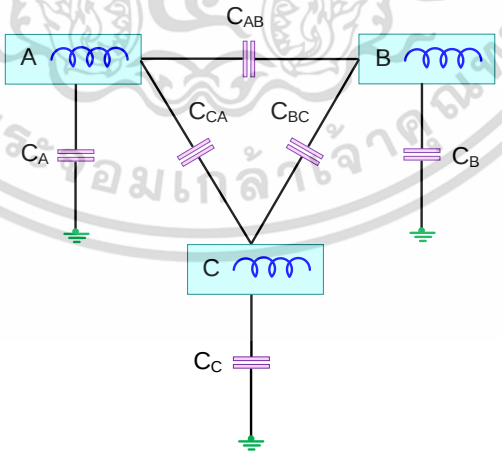

Fig. 3.1 Dielectric circuit for stator winding insulation [21].

The several measuring configurations of dielectric response measurement of the rotating machine were present as follows.

3.1.1 Individual phase to ground insulation

The configuration is when applying the voltage excitation to one phase while the other two phases are grounded. In this configuration both insulation parts i.e., phase-to-ground insulation (C_A) and interphase insulations (C_{AB} and C_{AC}) are under test as in Fig. 3.2.

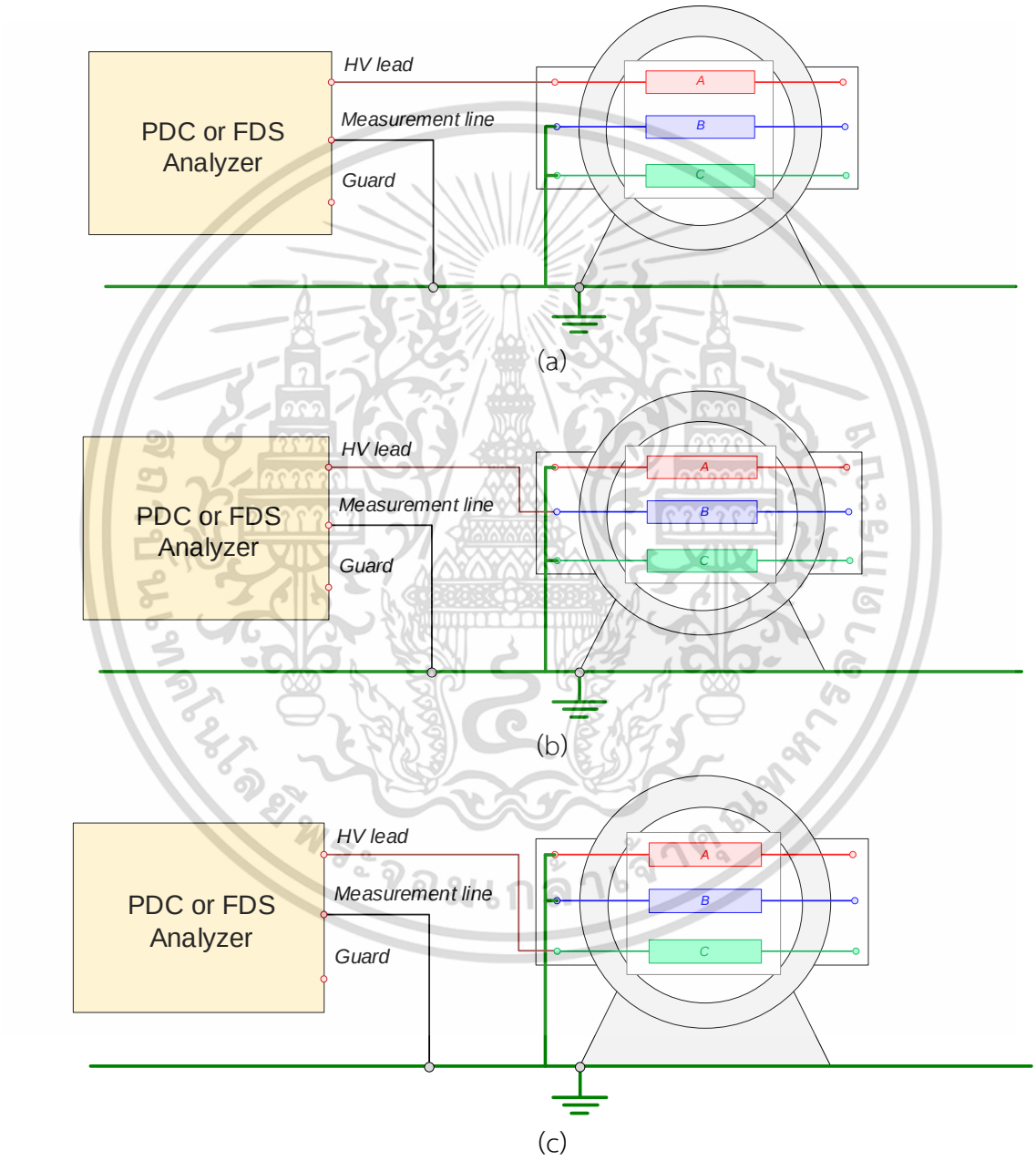

Fig. 3.2 Measuring configuration for individual phase to ground insulation (a) phase A (b) phase B and (c) phase C.

3.1.2 Entire phase to ground insulation

The configuration is when applying the voltage excitation to all three phases as in Fig. 3.3. In this configuration both insulation parts i.e., overall, three phases to ground insulation ($C_{AG}+C_{BG}+C_{CG}$) are under test. The information on the interphase insulations is not given in this case. This configuration is usually seen in the machine where the star point cannot be dismantled or when required to check the overview of the insulation only.

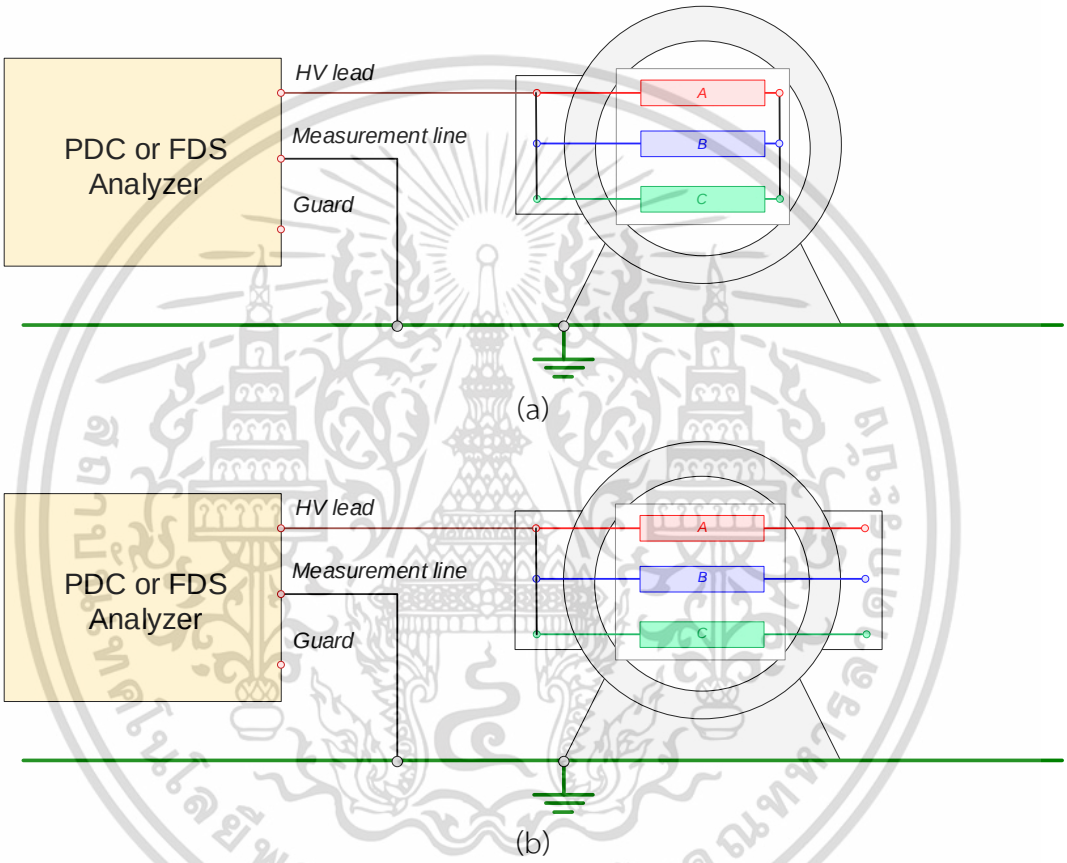

Fig. 3.3 Measuring configuration for entire phase to ground insulation
(a) machine with an inaccessible star point (b) machine with an accessible star point.

3.1.3 Phase-to-phase insulation

The configuration is when applying the voltage excitation to one phase and measuring the current at another phase, the remaining phase are ground. In this configuration, the interphase insulation and the series of phases to ground are under test as in Fig. 3.4. The configuration requires a floating test instrument i.e., voltage source and current are floating from the ground as in Annex D according to IEC 60034-27-4 [12]. This configuration is a “supplementary” test for insulation assessment of

rotating machines if the available time is limited or if the PDC measurement results of individual phase-to-ground insulation do not shown a significant level of leakage current.

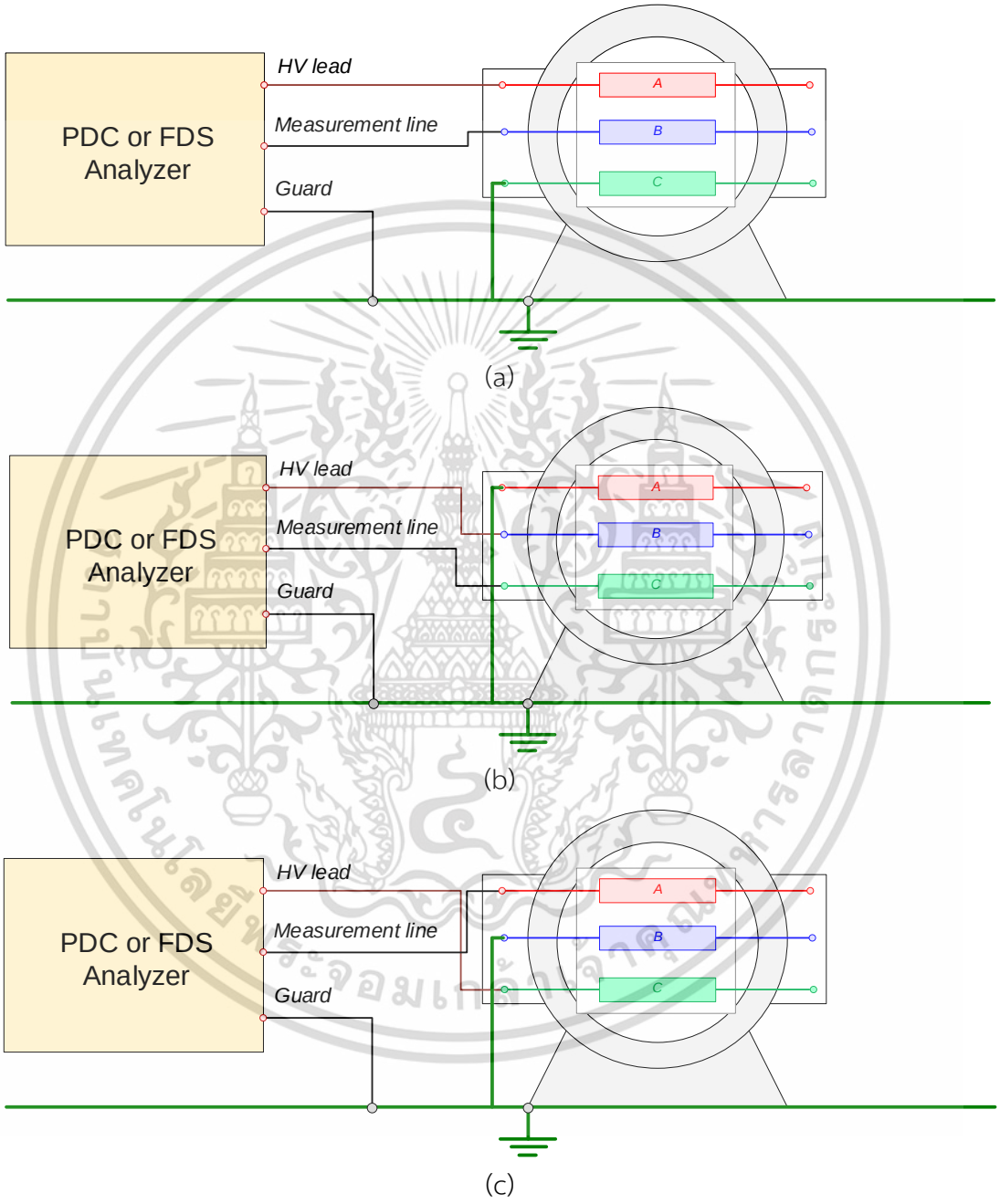

Fig. 3.4 Measuring configuration for individual phase-to-phase (interphase) insulation (a) phase A and B (b) phase B and C and (c) phase C and A.

3.2 Preparation before test

Before conducting the dielectric response measurement in either field or even laboratory. The

1. Discharge by grounding the insulation before performing the test: since in the case of PDC measurement the remaining charges stored in the insulation may affect the test as an off set of measurement results. Such charges stored were due to the equipment suddenly shut down or the insulation being tested by another person i.e., the Megger test. Thus, the insulation should be discharged by short-circuiting the terminals of the machine with the ground for sufficient time.
2. Record the status of machines to be tested e.g., insulation technology of machine (Epoxy-mica, polyester, etc.), manufacturing process (VPI, Resin rich), and so on.
3. Record the environmental parameters before- and during the test as follows.
    - **Ambient temperature**: ambient temperature is a critical parameter that can affect the test results. For instance,
    - **Stator winding temperature**: this parameter affects the test result since the dielectric response parameters e.g., conductivity and permittivity are functions of temperature. Thus, temperature correction is needed to treat the data before analysis. For rotating machine insulation, the correction temperature to 40 °C should be noticed [11].
    - **Relative humidity:** if the machine is open air type which exposes the external ambiance, the moisture in the air can adsorb over the surface of the stator winding insulation increasing leakage as conduction current component leading to misinterpretation.
    - Other necessary environmental information during the test.

3.3 Test procedures

3.3.1 PDC measurement test procedures

For an accurate measurement, it is necessary to determine the initial condition of the test object before any application of excitation voltage. The test procedure for performing the PDC measurement consisted of a three-step process are as follows [26]:

1. **Initial measurement**: this was made to determine the initial condition of the insulation system. The initial condition (or charging state) of a test object can be determined by monitoring the initial current which flows through it. For visualization of this current, it is sufficient to start a current measurement with a polarization duration of zero seconds. It is important that the initial current is low and at least in a steady state. In case of a high, but constant amplitude of initial current, this current can be considered as an "offset" for the evaluation: it can be subtracted from the measurements.
2. **Control measurement**: The control measurement procedure was conducted to confirm that there were no abnormalities in the PDC test circuit. Before starting the main measurement, it is recommended to carry out control measurements with a short charging duration e.g., 5-10 seconds to control the whole setup. Verify the amplitudes of measured currents and the value of the capacitance. Such a short control measurement will not affect the main measurement, because the relaxation currents induced by a short charging duration can be neglected after a few minutes of waiting time.
3. **Main measurement**: The main measurement can be performed after the control measurement by choosing adequate values for the charging voltage amplitude and for the duration of polarization and depolarization.

3.3.2 FDS measurement test procedures

For FDS measurement, since the effect of the remaining charge might be less significant, measuring the remaining charge (or current) is not needed. However, from a safety perspective, discharge by the grounding of the machine is required. Besides, this method can measure the impedance or complex capacitance of the insulation. Therefore, the capacitance at power frequency can be measured directly.

3.4 Dielectric response measurement results and analysis

3.4.1 Normalized current by dividing with the capacitance

The PDC measurement results were plotted on a log-log scale. Besides, the PDC measurement can compare between different machines and can be normalized by dividing with the capacitance C as follows:

$$i_{pol,norm}(t) = \frac{i_{pol}(t)}{C} \tag{3.1}$$

$$i_{dep,norm}(t) = \frac{i_{dep}(t)}{C} \tag{3.2}$$

The normalized current allows the comparison between complete machine winding or even individual coils or bars in the laboratory [17].

3.4.2 Transformation into frequency domain data

Besides the PDC measurement results in the time domain, it can be converted into the frequency domain for further analysis. The dielectric response in the frequency domain is the dielectric dissipation factor (DDF) which is used to investigate the characteristic and frequency dispersion of the DDF which could be changed over service life as aging or degradation mechanisms.

Extended Debye model was used as a model to convert parameters in the time domain into the frequency domain as follows [6].

$$\tan\delta(\omega) = \frac{\frac{1}{\omega R_{dc}} + \sum_{i=1}^{n} \frac{\omega R_i C_i^2}{1+(\omega R_i C_i)^2}}{C_{geo} + \sum_{i=1}^{n} \frac{C_i}{1+(\omega R_i C_i)^2}} \tag{3.3}$$

where C_{geo} is the high-frequency capacitance or geometric capacitance, R_{dc} is the DC resistance, R_i and C_i is the series resistance and capacitance, representing dielectric loss due to the slow process of polarization phenomena. The following parameters were obtained by the nonlinear curve fitting technique.

On the other hand, the DDF can be calculated using “Hamon approximation” [27] as the equation below.

$$\tan\delta = \frac{i(t)}{2\pi f U_c C} \tag{3.4}$$

where $i(t)$ is polarization current $i_{pol}(t)$ or depolarization current $i_{dep}(t)$, $t = 0.1/f$.

From equation (3.4), if the polarization current $i_{pol}(t)$ was used, the DDF or $\tan\delta$ will be comprised of either the polarization loss component or a conduction loss component. While if depolarization current $i_{pol}(t)$ was used, the DDF or $\tan\delta$ will be a polarization loss component.

3.5 Case studies

In this thesis, generators and motors are investigated as detailed in Table 3.1.

Table 3.1 Details of case studies

Case studies	Machine	Rating	Dielectric response Measurement		Description
			PDC	FDS	
1	Generators	50 MVA, 11.5 kV	✓		Comparison between two generators with identical rates and type
2	Motors	2.3 MW. 6.6 kV	✓	✓	Effect of contamination of two motors
3	Motor	250 kW, 6.9 kV	✓		Measurement before and after drying and cleaning process
4	Motor	2.5 MW, 6.9 kV	✓		Healthy stator winding insulation condition
5	Motor	2.8 MW, 6.9 kV	✓		Motor with a high level of partial discharge magnitude

Chapter 4

Test Results and Discussion

In this chapter, on-site experiments of dielectric response measurements on several machines were conducted. Test results were analyzed and discussed.

4.1 Case study 1: PDC measurement on two 50 MVA, 11.5 kV Air-cooled generators

In the experiment, PDC measurements were conducted on the stator winding insulation of two generators, which have the same rate of 50.8 MVA, and 11.5 kV in the power plant (temperature 30-35 °C, 60-70 %RH). Two investigated generators were labeled generator A and generator B, respectively. This case study based on the author's work has been published in [28]. Fig. 4.1 shows one of the generators to be investigated.

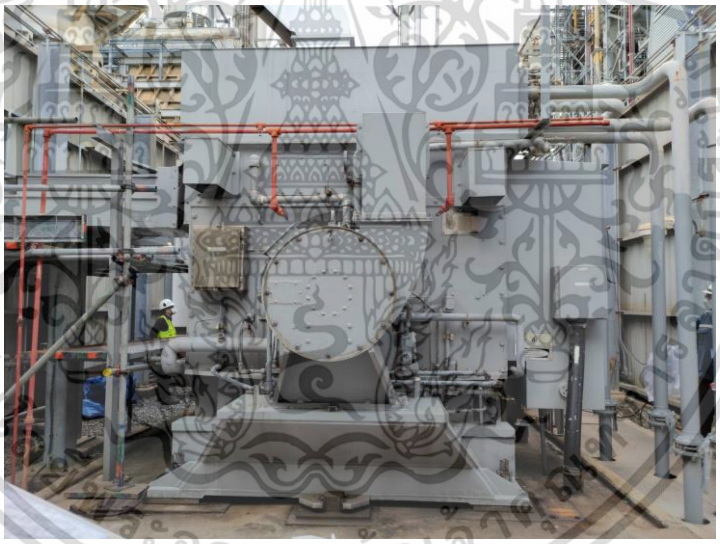

Fig. 4.1 Investigated generator of case study 1.

The PDC results of the phase-to-ground insulation of the two investigated generators were normalized by dividing the currents with the capacitance of the stator winding insulation to allow the comparison in between, as shown in Fig. 4.2. The capacitance of the phase-to-ground insulation of the stator winding of the two investigated generators was about 190 nF. Since the PDC results in each phase were similar, only a single phase (phase A) of the PDC results of the test circuit of individual phase to ground insulation to compare the PDC characteristics of identical rated machines.

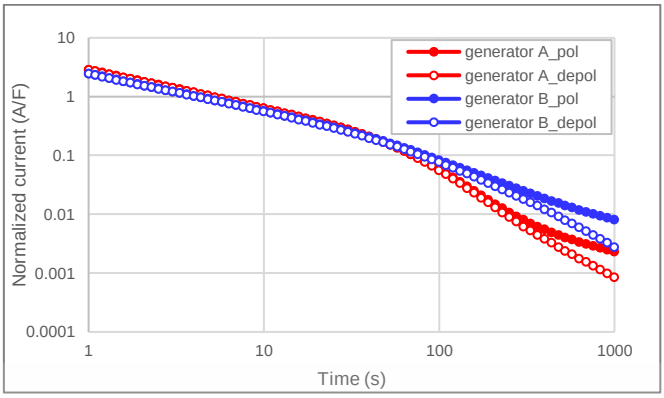

Fig. 4.2 Normalized PDC measured from the individual phase to ground insulation.

The PDC results of phase-to-phase insulation of the two investigated generators are illustrated in Fig. 4.3. The capacitance of the interphase insulation of the stator winding of the two investigated generators was about 1 nF. As the same for phase-to-ground insulation, since the PDC results in each dual phase were similar, only a single dual phase (Phase A and B) of the PDC results of phase-to-phase was collected to introduce.

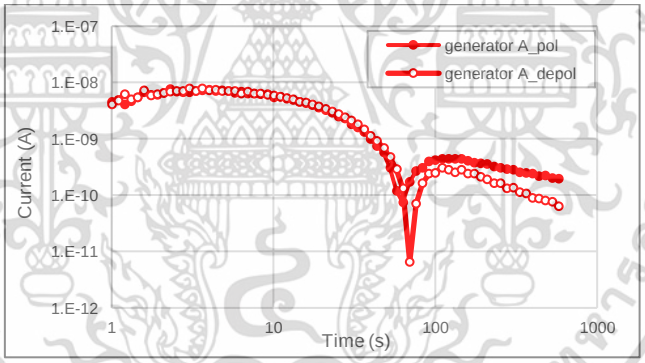

(a)

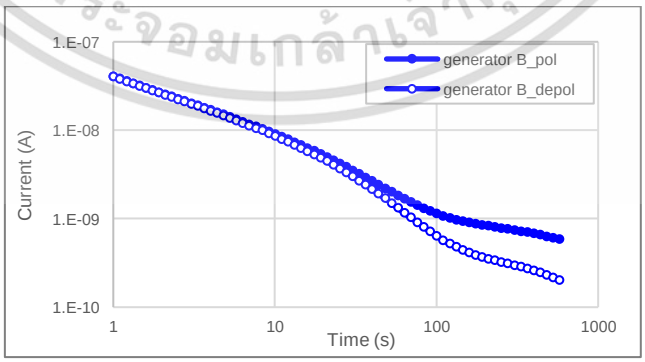

(b)

Fig. 4.3 PDC measured from the phase-to-phase insulation of (a) generator A (b) generator B.

The polarization and depolarization current curves of two generators measuring from the phase to ground insulation represent the “hump” in the time between 10-100 s, i.e., relaxation peak in the dielectric loss factor curve in the frequency domain between 1-10 mHz. Since the hump shape was observed in the polarization current curve, a high value of PI was reported. The PI values of generator A and generator B were 34 and 11, respectively. Such a high value of PI was strongly influenced by the stress grading control of the stator winding insulation system [11, 17]. Considering the polarization current curve, the current between the time of 100-1000 s shows a “bending curve”, accordingly, resulting in a lower current and a higher IR at the time of 600 s. This hump was caused by the influence of the stress grading control system having non-linearity characteristics [11].

The PDC curves of generator A measuring from the phase-to-phase insulation, as shown in Fig. 4.3(a), represent the polarity reversal (or Anomalous current) of both polarization and depolarization current at the time of about 60-70 s. Such polarity reversal also causes the reverse of the DDF in the frequency domain. Reference [29] reported that when performing the power factor test on the interphase insulation of the stator winding insulation of the generator using the test circuit configuration similar to the phase-to-phase insulation for measuring interphase insulation in this experiment, it is possible to obtain the negative value of power factor (also DDF). It causes when the power factor of the interphase insulation is a lower influence when compared with that of phase-to-ground insulation [29]. Accordingly, the DDF of generator A, as illustrated in Fig. 4.4, was relatively low (compared with the DDF of generator B), so it can be implied that the power factor (or DDF in this case) was lower when compared with that of phase-to-ground insulation. However, the test circuit for measuring the PI and IR (also PDC measurement) of interphase insulation in IEC 60034-27-4 used a float test instrument to measure [12]. From such a circuit configuration, the guard electrode is not needed.

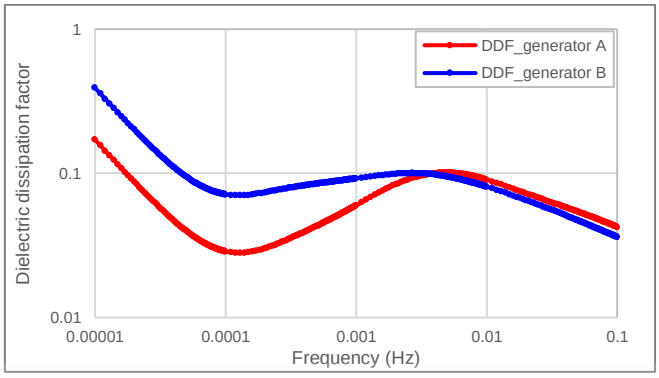

Fig. 4.4 DDF of phase-to-ground insulation of two investigated generators.

In the case of generator B, polarization and depolarization current curves revealed the hump shape as seen in the polarization and depolarization curve of phase-to-ground insulation. Besides, both polarization and depolarization currents were not reversed. The results exhibit more significance on the dielectric loss of the interphase insulation than that of the phase-to-ground insulation.

4.2 Case study 2: PDC and FDS measurement on two 6.6 kV Motors

Two MV motors are operated together as boiler-feed water pumps. During an outage for preventive maintenance, the enclosure was opened for visual inspection of the stator winding part. As can see in Fig. 4.5, the endwinding region of both MV motors is contaminated with dust, motor B seems to have a higher degree. Thereafter, the dielectric response measurement (DRM) in the time domain was performed to evaluate the insulation condition of the stator winding.

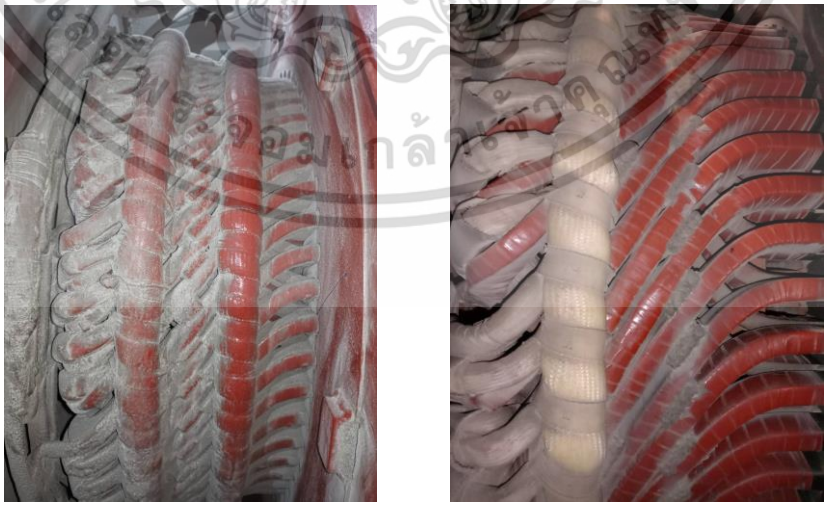

(a) (b)

Fig. 4.5 Representation of the contamination over the endwinding surface of (a) motor A (b) motor B.

The PDC results of motor A before cleaning are shown in Fig. 4.6. It was undoubtedly a high level of the conductive current component, which reveals quite difference in polarization and depolarization current. The PI value subtracted from the polarization current of this motor was 2.60.

Thereafter, the stator winding insulation was cleaned with solvent and the DRM was re-measured again. It was found that a higher level of currents is given. It was probably caused by a little moisture ingress in the bulk insulation, in which dipolar molecules of moisture or water yield higher loss due to dipolar polarization in the higher frequency range. The PI value subtracted from the polarization current of this motor after cleaning is 3.02. From this, it is well known that the PI value is calculated by the quotient of polarization current at 1 min and 10 min. Thus, if we consider the PDC shape, it can be found that the increasing PI value does not mean that the polarization current at 10 min decreases but because of polarization current at 1 min increases. Concisely, in this case, increasing in the PI value did not always mean that the insulation condition was better.

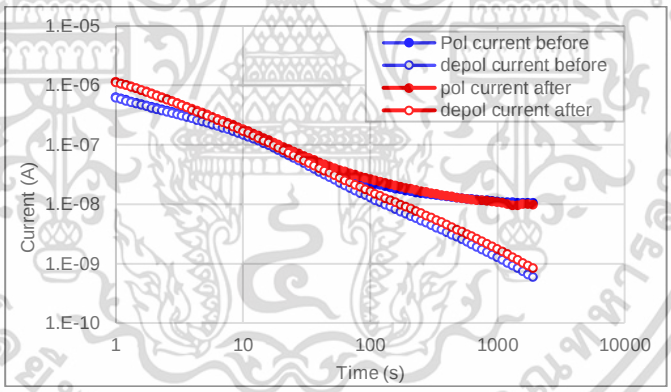

Fig. 4.6 PDC of motor A before and after.

Furthermore, the PDC results of motor B as shown in Fig. 4.7, seem to be the conductive current component, greatly higher than that of motor A. From the test results, it was assumed that motor B has been contaminated with moisture adsorption at a higher level. Such moisture ingress can cause a conductive path to allow the current to flow through the grounded stator core. The PI value subtracted from the polarization current of this motor is just 1.05. After investigation, the operator found problems with the heater of the motor and decide to on-site heat the stator winding for drying out.

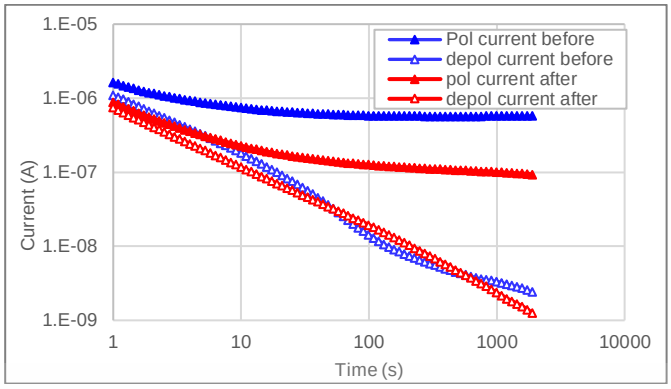

Fig. 4.7 PDC of motor B before and after cleaning and drying.

After the drying process overnight, the PDC was re-measured. Unsurprisingly, the PDC results revealed that the polarization current was reduced by about an order of magnitude since the moisture content as a conductive media, dries out over time. Besides, The PI value subtracted from the polarization current of this motor was increased to 1.30. However, there still reveals the high level of conduction current component, i.e., the drying process was still incomplete. Therefore, more time for the drying process is required before returning to service. Unfortunately, the author has no opportunity to re-measure again due to time constraints.

Considering the depolarization current as shown in Fig. 4.8, it was found that both motors reveal the depolarization current with nearly the same trace and level. From this, it was implied that the moisture ingress is almost only over the surface of the endwinding region. Since the depolarization current only represents the polarization loss in the bulk insulation. By which the conduction current component is not integrated into the depolarization current since the component is only present during voltage is applied.

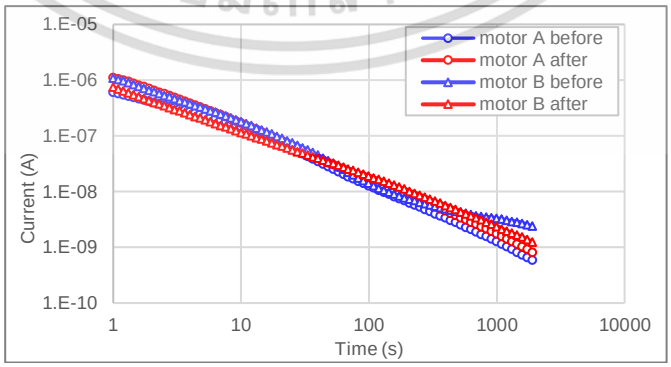

Fig. 4.8 Depolarization currents of motor A and motor B.

Typically, if desires to compare the result with another one machine or even a stator coil in the laboratory, the currents should be normalized by dividing currents with the capacitance of the insulation for comparison aspect [17]. However, the capacitance measured of both MV motors is close (the capacitance of both motors was about 220-230 nF).

Besides the PDC measurement, the FDS was also performed on both motors. In Fig. 4.9, although the stator winding was cleaned, the DDF trace did not have a reduced value. From this, a higher level of DDF trace in case after cleaning is due to the measurement being done a few days later, hence the moisture might ingress onto and into the insulation in the meantime. Also, in Fig. 4.10 although the visual inspection evidence that the lower level of dust deposited in the endwinding region, the DDF trace exhibits an even higher level compared with that of motor A. In this case, moisture absorption over the surface insulation was greatly affected as can be found in the considerably high conduction loss component contributed to the DDF.

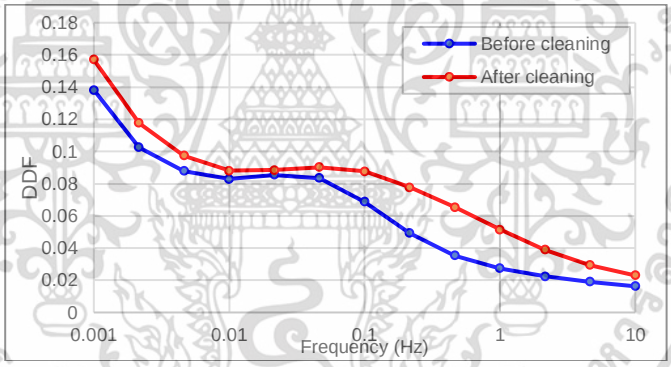

Fig. 4.9 FDS of motor A before and after cleaning.

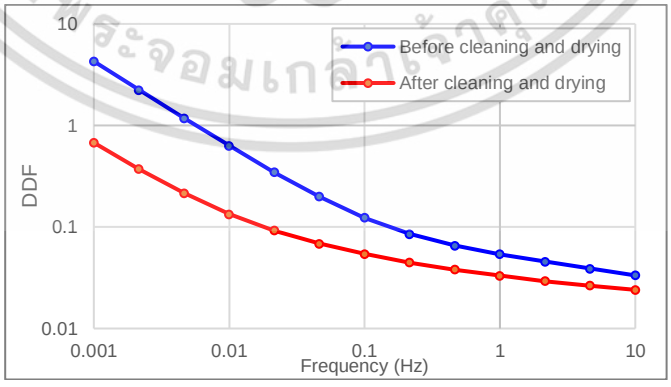

Fig. 4.10 FDS of motor B before and after cleaning and drying.

From the visual inspection, it seems that motor A was more severe with contaminants than that of motor B, which did not produce consistent with PDC and

FDS test results. As the test results show that motor B has a high degree of conduction component which could be described by the effect of moisture absorption in the case of motor B due to the malfunction of the heater while motor A experiences with amount of dust with less conductive properties. Moreover, the depolarization currents, which is directly proportional to the polarization loss in the bulk insulation, of both motors reveal that the moisture absorption in the bulk was less significant, i.e., the moisture absorption was mainly on the endwinding surface.

4.3 Case study 3: PDC measurement on 250 kW, 6.9 kV Motor before and after cleaning and drying

This experiment was conducted during time-based maintenance of a 250 kW, 6.9 kV motor. The PDC measurements were performed either before or after the cleaning and drying process. The investigated motor and PDC test arrangements are illustrated in Fig. 4.11.

(a)

(b)

Fig. 4.11 (a) Investigated motor of case study 3 (b) PDC measurement at site.

In this case study, since the neutral point is inaccessible and cannot dismantled, PDC measurement was only done on the entire phase of the stator winding. The PDC measurement results are shown in Fig. 4.12.

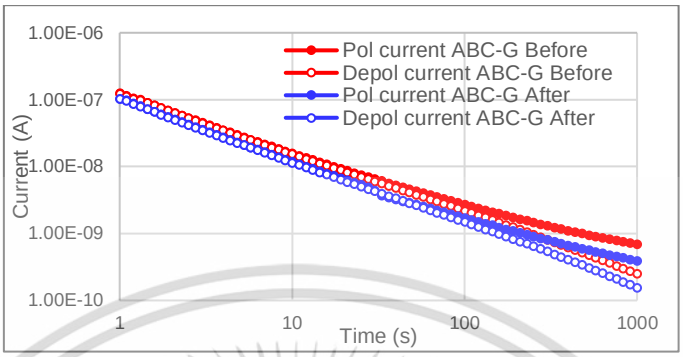

Fig. 4.12 PDC measurement results of case study 3.

Subsequently, the PDC measurement results were converted into the frequency domain using Hamon approximation as the DDF parameter as shown in Fig. 4.13.

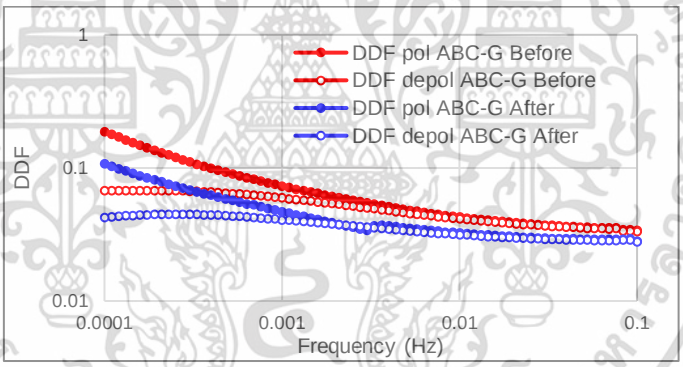

Fig. 4.13 DDF of case study 3.

From the test results above, it was clearly found that the after cleaning and drying process, either polarization or depolarization currents were diminished. Unsurprisingly, since the conductive contamination over the surface of the stator winding as a source of conduction component contributed to the polarization current was cleaned and dried, thus, resulting in the reduction of the overall polarization current as can also be found in the DDF trace (DDF converted from polarization current). Moreover, as the depolarization current mainly refers to the loss in the bulk insulation, the moisture trapped in the insulation also dried out resulting in the reduction of depolarization current as can also be found in the DDF trace (DDF converted from depolarization current).

4.4 Case study 4: PDC measurement on 2.5 MW, 6.9 kV Motor

This experiment was conducted during time-based maintenance of a 2.5 MW, 6.9 kV motor. The PDC measurements were performed after the cleaning and drying process. The investigated motor and PDC test arrangements are illustrated in Fig. 4.14. This case study intended to demonstrate the stator winding of the motor having acceptable conditions in either “integral” or “local” conditions.

Fig. 4.14 (a) Investigated motor of case study 3 (b) PDC measurement at the workshop.

The PDC measurement results are shown in Fig. 4.15. In this case study, the neutral point of this motor can be dismantled which enables to perform the experiment on each phase. As the PDC measurement results of each phase are similar, thus, only phase A was collected to present. Besides, the PD measurement was also conducted on this motor. The PD measurement results revealed an internal delamination pattern with an acceptable level of magnitude i.e., about 1-2 nC.

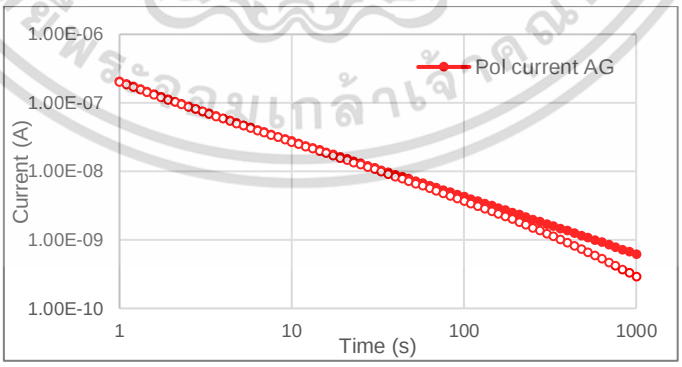

Fig. 4.15 PDC measurement results of case study 4.

Subsequently, the PDC measurement results were converted into the frequency domain using Hamon approximation as the DDF parameter as shown in Fig. 4.16.

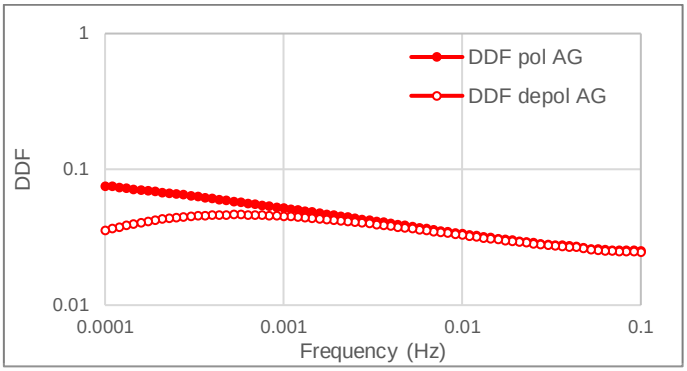

Fig. 4.16 DDF of case study 4.

From the PDC measurement results, it was found that this motor was in normal condition with a low conductive contribution, as can be seen in superimpose of both polarization current and depolarization for about two decades. Besides, considering the depolarization current and also its DDF converted from depolarization current, which refers to polarization loss in the bulk insulation, exhibit low loss.

4.5 Case study 5: PDC measurement on 2.8 MW, 6.9 kV Motor

This experiment was conducted during time-based maintenance of a 2.8 MW, 6.9 kV motor. The PDC measurements were performed after the cleaning and drying process. The investigated motor and PDC test arrangements are illustrated in Fig. 4.17.

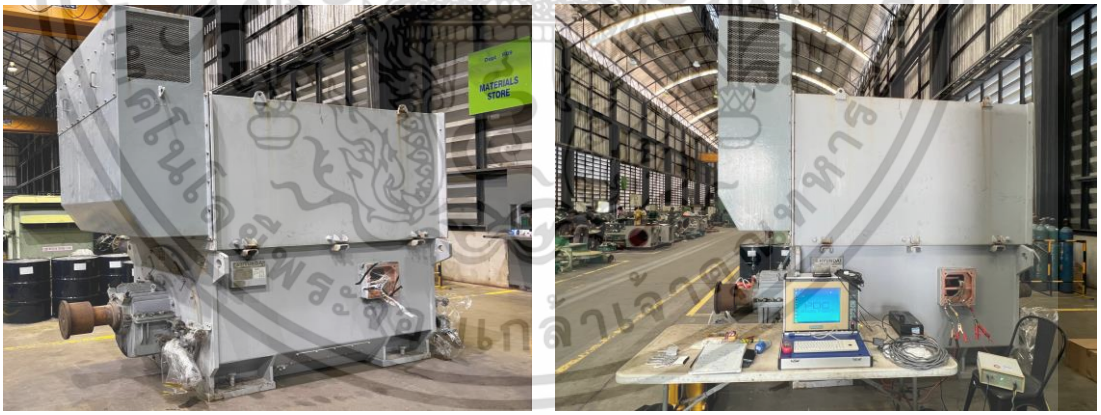

(a) (b)

Fig. 4.17 (a) Investigated motor of case study 5 (b) PDC measurement at the workshop.

The PDC measurement results were shown in Fig. 4.18. In this case study, the neutral point of this motor can be dismantled which enables to perform the experiment on each phase.

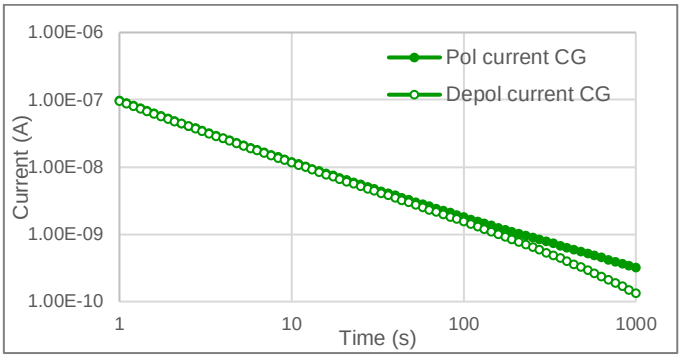

Fig. 4.18 PDC measurement results of case study 5.

Subsequently, the PDC measurement results were converted into the frequency domain using Hamon approximation as DDF parameter as shown in Fig. 4.19.

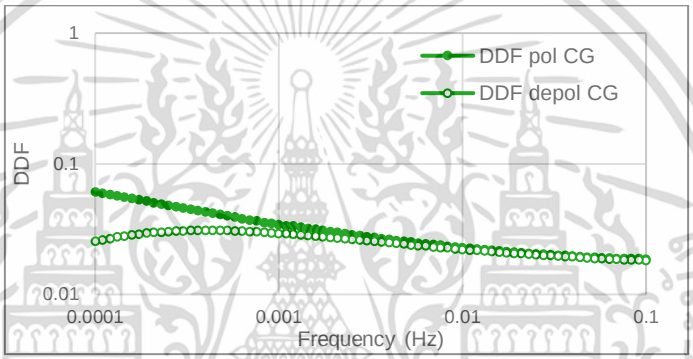

Fig. 4.19 DDF of case study 5.

From the PDC measurement results, it was found that this motor was in normal condition with a low conductive contribution, as can be seen in superimpose of both polarization current and depolarization for two decades. Besides, considering the depolarization current and also its DDF converted from depolarization current, which refers to polarization loss in the bulk insulation, exhibit low loss.

However, considering the PD measurement result of this motor as shown in Fig. 4.20, a noticeably high level of the PD magnitude up to 30 nC was given, offering a serious problem with the stator winding.

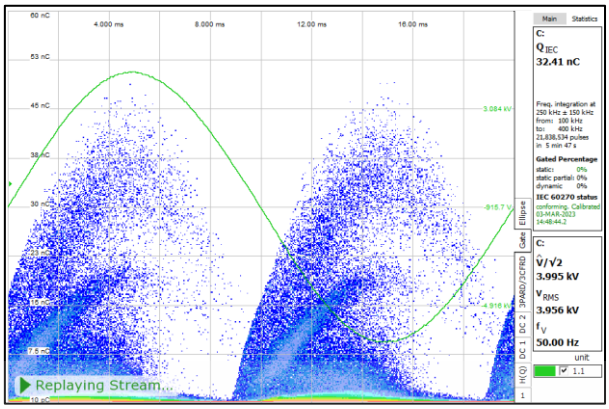

Fig. 4.20 Partial discharge test results of this motor (phase C).

In the case of critical machines, a particularly high level of PD magnitude cannot be acceptable for the reliability of service. In this case study, the PDC measurement results were not produced consistently with the PD measurement. Therefore, only dielectric response measurement that can determine the only integral insulation, cannot be sufficient to assess the overall insulation condition of the rotating machine.

Chapter 5
Summary

5.1 Summary

From the measurement results in Chapter 4, it can be summarized each case study is as follows.

5.1.1 Case study 1

This case study demonstrated the comparison of two generators with identical rates and types. The PDC measurement results of phase-to-ground insulation exhibit relatively high values of PI on both generators. A particular effect was a result of the stress grading material having non-linear resistance characteristics resulting in an interfacial polarization loss peak. Besides, PDC measurements on the phase-to-phase insulation that has also been performed, exhibit the anomalous current or polarity reversal characteristic. From this, it can be concluded that a particular effect may be caused by less influence of the loss factors of the phase-to-phase insulation compared with that of phase-to-ground insulation.

Regarding dielectric response measurement on the phase-to-phase insulation, this test configuration should be a “supplementary” test i.e., if the results gathered from the phase-to-ground measurement did not show any abnormalities, thus, the phase-to-phase insulation measurement is not needed and also when the operating time (for measurement) was limited, because only the phase to ground measurement results could provide sufficient information to evaluate the insulation condition.

5.1.2 Case study 2

This case study demonstrated the effect of the contamination on the stator winding of two motors. In this case study, the PDC and FDS measurements were conducted on both motors. Test results showed how moisture affects the dielectric response measurement which can be seen in extremely high polarization current in motor B as the malfunction of the heater. A particular high polarization current is attributed to the conduction current component as moisture absorption on the endwinding surface. While in the case of motor A, even the visual inspection represents a high degree of visible contamination, the PDC results just reveal a quite high

polarization current and lower compared with that of motor B. Thus, it was assumed that such contamination had low conductive properties. However, from the depolarization current of both motors, it was revealed that moisture can partly ingress in the bulk insulation. Besides, the FDS results of the motor with moisture contamination predominantly exhibit a conduction loss factor that overwhelms all dielectric loss factors, from this, it was difficult to expose the polarization loss that refers to the condition of the bulk insulation.

From the case study, it was found that the PDC measurement was an effective way to flexibility investigate the insulation in the bulk or even surface condition when compared with the FDS measurement.

5.1.3 Case study 3

This case study demonstrated the effect of the cleaning and drying process during time-based preventive maintenance. The PDC results show an improving insulation condition in both bulk and surface insulation.

5.1.4 Case study 4

This case study revealed the PDC measurement results of a motor that is in a healthy integral insulation condition. This case study can be used as reference data for stator winding with acceptable integral conditions, to create the database for assessing the stator winding insulation.

5.1.5 Case study 5

From the test results, it can be concluded that the PDC test results did not produce consistent with PD test results. Since the PDC results revealed the stator winding insulation condition was acceptable. This case study demonstrated that only a single measurement technique is not enough sensitivity to judge the condition of the insulation. Therefore, more test techniques are recommended i.e., techniques that cover either “integral” or “local” conditions, in order to get the complete insulation assessment of the stator winding insulation of rotating machine. However, in practice, it is not just about the engineering aspect alone but must also take into account the economic aspect and suitability.

From the experiment, it can be summarized that the PDC and FDS measurements as dielectric response measurements can be valuable tools for assessing the integral condition of the stator winding insulation of rotating machine.

For rotating machine insulation, the DRM in the time domain is preferred for being the effective method for evaluating the insulation condition. On the one hand, there is still necessary to analyze the frequency domain. However, the current response can be converted into the DDF in the frequency domain to allow the analysis as an alternative way.

5.2 Further research recommendation

There are some recommendations associated with the investigation of the stator winding insulation of the rotating machine as follows.

- Artificial simulation of the various stresses on stator coils, and bars should be done, as reference information for assessing the stator winding insulation of rotating machines in the real world.
- More test experiments are needed to gather information as a database to propose standardized for dielectric response measurement of rotating machines.
- Other techniques i.e., partial discharge test, dissipation factor, or tip-up should be combined to complete the stator winding insulation assessment.
- The application of very low frequency (VLF) test voltage on rotating machines, in either PD or dissipation factor diagnostic, is of interest. Thus, more study is needed.

References

[1] G. C. Stone, E. A. Boulter, I. Culbert, and H. Dhirani, “Electrical Insulation for Rotating Machines,” 1st Ed., Wiley-IEEE Press, 2004.

[2] W. McDermid, "Insulation systems and monitoring for stator windings of large rotating machines," in IEEE Electrical Insulation Magazine, vol. 9, no. 4, pp. 7-15, July-Aug. 1993

[3] IEEE Std 56-2016, "IEEE Guide for Insulation Maintenance of Electric Machines,".

[4] Andreas Küchler. High Voltage Engineering Fundamentals-Technology-Applications. Germany : Springer-Verlag GmbH. 2018.

[5] E. Kuffel, W.S. Zaengl, and J. Kuffel, High Voltage Engineering: Fundamentals. Butterworth-Heinemann, Second edition 2000

[6] W. S. Zaengl, "Dielectric spectroscopy in time and frequency domain for HV power equipment. I. Theoretical considerations," in IEEE Electrical Insulation Magazine, vol. 19, no. 5, pp. 5-19, Sept.-Oct. 2003.

[7] W. S. Zaengl, "Applications of dielectric spectroscopy in time and frequency domain for HV power equipment," in IEEE Electrical Insulation Magazine, vol. 19, no. 6, pp. 9-22, Nov.-Dec. 2003.

[8] V. Der Houhanessian, “Measurement and analysis of dielectric response in oil-paper insulation systems,” Ph.D. thesis, Swiss Federal Institute of Technology, No. 12832, Zurich, 1998.

[9] K.C. Koa, Dielectric Phenomena in Solids: with emphasis on physical concepts of electronic process, Elsevier Academic Press, 2004, pp. 52-90.

[10] CIGRE Technical Brochure 558, “Guide for the Monitoring, Diagnosis and Prognosis of Large Motors,” CIGRE: Paris, France, 2013.

[11] IEEE Std 43-2013 (Revision of IEEE Std 43-2000), “Recommended Practice for Testing Insulation Resistance of Electric Machinery”.

[12] IEC 60034-27-4:2018, “Rotating electrical machines - Part 27-4: Measurement of insulation resistance and polarization index of winding insulation of rotating electrical machines”.

[13] T. K. Saha and P. Purkait, "Investigation of polarization and depolarization current measurements for the assessment of oil-paper insulation of aged transformers," in

IEEE Transactions on Dielectrics and Electrical Insulation, vol. 11, no. 1, pp. 144-154, Feb. 2004.

[14] P. Birkner, "Field experience with a condition-based maintenance program of 20-kV XLPE distribution system using IRC-analysis," in IEEE Transactions on Power Delivery, vol. 19, no. 1, pp. 3-8, Jan. 2004.

[15] IEEE Std C57.161-2018, "IEEE Guide for Dielectric Frequency Response Test,".

[16] J. Cheng, N. Taylor and P. Werelius, "Nonlinear Dielectric Properties of the Stator and Transformer Insulation Systems," in IEEE Transactions on Dielectrics and Electrical Insulation, vol. 29, no. 1, pp. 240-246, Feb. 2022.

[17] E. David, R. Soltani and L. Lamarre, "PDC measurements to assess machine insulation," in IEEE Transactions on Dielectrics and Electrical Insulation, vol. 17, no. 5, pp. 1461-1469, October 2010.

[18] M. Farahani, H. Borsi and E. Gockenbach, "Dielectric response studies on insulating system of high voltage rotating machines," in IEEE Transactions on Dielectrics and Electrical Insulation, vol. 13, no. 2, pp. 383-393, April 2006.

[19] S. A. Bhumiwat, "On-site non-destructive dielectric response diagnosis of rotating machines," in IEEE Transactions on Dielectrics and Electrical Insulation, vol. 17, no. 5, pp. 1453-1460, October 2010.

[20] T. K. Saha and Zheng Tong Yao, "Experience with return voltage measurements for assessing insulation conditions in service-aged transformers," in IEEE Transactions on Power Delivery, vol. 18, no. 1, pp. 128-135, Jan. 2003.

[21] IEEE Std 286-2000, "IEEE Recommended Practice for Measurement of Power Factor Tip-Up of Electric Machinery Stator Coil Insulation,".

[22] OMICRON Lab Webinar Series “Dielectric Spectroscopy of Solid Insulators,” 2020.

[23] J. Blennow, C. Ekanayake, K. Walczak, B. Garcia and S. M. Gubanski, "Field experiences with measurements of dielectric response in frequency domain for power transformer diagnostics," in IEEE Transactions on Power Delivery, vol. 21, no. 2, pp. 681-688, April 2006.

[24] M. Koch and M. Kruger, "A fast and reliable dielectric diagnostic method to determine moisture in power transformers," 2008 International Conference on Condition Monitoring and Diagnosis, Beijing, China, 2008.

[25] CIGRE Technical Brochure 552, “Guide of methods for determining the condition of stator winding insulation and their effectiveness in large motors,” CIGRE: Paris, France, 2013.

[26] ALFF Engineering, “User’s Guide PDC-ANALYSER-1MOD,”.

[27] B. V. Hamon, “An Approximation Method for Deducting Dielectric Loss Factor from Direct-Current Measurement”, Proc. Inst. Elec. Eng. (IEE), Vol. 99, No. 27, pp. 151-155, 1952.

[28] S. Jeenmuang, P. Pannil, S. Mongkolsatitpong, S. Trakuldit, V. Wuti and N. Pattanadech, "The Application of Polarization and Depolarization Current on the Large Turbo-generators," 2022 9th International Conference on Condition Monitoring and Diagnosis (CMD), Kitakyushu, Japan, pp. 118-121, 2022.

[29] L. Pong, “Review Negative Power Factor Test Results and Case Study Analysis,” The 2002 Int. Conf. of Doble Clients; Boston/ USA, 2002.

Appendix

Appendix A

Research Article

Research Article

S. Jeenmuang, P. Pannil, S. Mongkolsatitpong, S. Trakuldit, V. Wuti and N. Pattanadech, "The Application of Polarization and Depolarization Current on the Large Turbo-generators," 2022 9th International Conference on Condition Monitoring and Diagnosis (CMD), Kitakyushu, Japan, 2022, pp. 118-121, doi: 10.23919/CMD54214.2022.9991272.

2022 9th International Conference on Condition Monitoring and Diagnosis (CMD)

Hybrid style

On-site participation at the Kitakyushu International Conference Center, Kitakyushu, Japan, and online participation

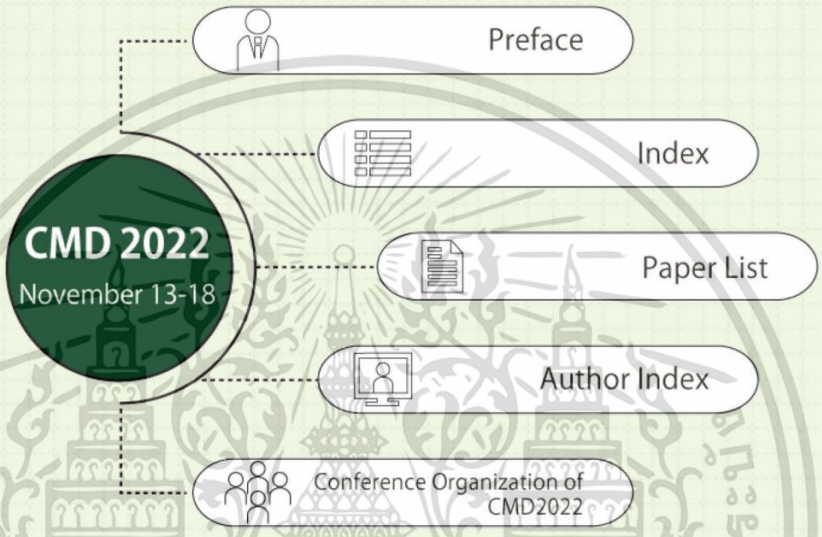

Download All Data

Sponsored by :
IEEJ Technical Committee on Dielectrics and Electrical Insulation

Technically co-sponsored by :
IEEE Dielectrics and Electrical Insulation Society

Supported by :
City of Kitakyushu
Kitakyushu Convention & Visitors Association
SECOM Science and Technology Foundation
The Institute of Electrical Installation Engineers of Japan, Kyushu Chapter
IEEJ, Kyushu Chapter

Published by Noboru Fujiwara
The Institute of Electrical Engineers of Japan
6-2 Gobancho, Chiyodaku, Tokyo 102-0076, Japan

ISBN 978-4-88686-431-4
IEEE Catalog Number: CFP2230D-ART

IEEE Meetings, Conferences & Events (MCE)
445 Hoes Lane Piscataway, NJ 08854 USA
Email: ieee-mce@ieee.org

B1-5

Conference Proceedings of CMD 2022

The Application of Polarization and Depolarization Current on the Large Turbo-generators

S. Jeenmuang[1*], P. Pannil[2], S. Mongkolsatitpong[3], S. Trakuldit[4], V. Wuti[5] and N. Pattanadech[1]
[1] Department of Electrical Engineering, School of Engineering, King Mongkut's Institute of Technology Ladkrabang, Bangkok, Thailand
[2] Department of Instrumentation and Control Engineering, School of Engineering, King Mongkut's Institute of Technology Ladkrabang, Bangkok, Thailand
[3] Plan Market Gold Co., Ltd and PD Solution Co., Ltd., Bangkok, Thailand
[4] Faculty of Industrial Technology, Nakhon Si Thammarat Rajabhat University, Nakhon Si Thammarat, Thailand
[5] School of Engineering, King Mongkut's Institute of Technology Ladkrabang, Bangkok, Thailand
*E-mail: 64601140@kmitl.ac.th

Abstract **–This paper represents the application of the polarization and depolarization current (PDC) measurement of the stator winding insulation of two large turbo-generators, which have the same rate of 50.8 MVA, and 11.5 kV. The PDC measurements were conducted on the stator winding insulation of both generators by using two different test circuits i.e., (individual) phase-to-ground insulation and interphase insulation circuits. Then, the PDC results of the two investigated generators were compared. To evaluate the phase-to-ground insulation condition of the stator winding insulation of both generators, the conventional dielectric parameters in the time domain, such as polarization index and insulation resistance, were also studied. Moreover, the PDC results in the time domain were converted into the dielectric dissipation factor in the frequency domain to allow the analyzing the phase-to-ground insulation of the stator winding of the generators. The PDC results of the phase-to-ground insulation circuits of both investigated generators illustrate the bent shape of PDC results which were affected by the influence of the stress control coating resulting in a high value of the Polarization index. Besides, the PDC results of the interphase insulation circuits of the first investigated generator illustrate the polarity reversal (or Anomalous current) of both PDC, while the second investigated generator illustrates the non-polarity reversal of both PDC. The polarity reversal of the PDC results of the interphase insulation was due to the dielectric loss of the interphase insulation is a lower influence when compared with that of phase-to-ground insulation.**

Keywords: turbo-generator, PDC, stator winding, polarization index, dielectric dissipation factor

I. INTRODUCTION

Generator is a vital asset in a power generation section that is operationally utilized in power plants that produce electrical energy into power systems. Particularly, turbogenerator is frequently found in gas and coal power plants. Practically, in operation, the insulation of the generator can encounter various stresses, i.e., Thermal, Electrical, Ambient (or Atmosphere) and Mechanical, also known as TEAM stresses, resulting in insulation degradation [1]. Such stresses are mainly presenced simultaneously as combined stress which accelerates aging of the stator winding insulation of the generator. Indeed, thermal stress can occur in the insulation system of the generator due to the load current flowing through the copper conductor of stator winding resulting in heat loss or so-called I^2R loss, which may not dissipate into the external ambient. Such problems may be caused by the dust or contamination having low-thermal conduction properties accumulated in the slot portion, resulting in the hot spot in the insulation system yielding the delamination in the stator winding insulation system e.g., between the copper conductor and groundwall insulation, delamination in the groundwall insulation and interfaces between stress control grading system. Mechanical stress can be caused by the vibration of the stator winding due to magnetic force. Regarding ambient stress, the groundwall insulation can partly absorb the humidity, or it can condense as water film over the overhang region.

Polarization and depolarization current (PDC) measurement is one of the DC methods to assess the insulation condition of various apparatus used in the power system, such as power transformers and rotating machines [2]. More information of the dielectric response of the insulation system is almost completely provided when using PDC measurement that continuously measures both polarization current and depolarization current instead of traditional measurement, i.e., polarization index (PI), insulation resistance (IR), which only measure the polarization current at one or two points [3]. However, both PI and IR are still used as basic parameters that can primarily assess the insulation condition of the rotating machine. For instance, if the contamination such as dust or bearing oil were presented on the endwinding surface, it can yield a lower PI value i.e., close to 1 [4]. On the other hand, in case of the groundwall insulation that was thermally stressed in [4], a higher PI value may be given. Besides, the dielectric model of the insulation systems can be drawn by using the curve-fitting technique to obtain the parameters that can represent the dielectric model. Thereafter, the parameters in the time domain from PDC result can be converted into the parameters in the frequency domain i.e., dielectric dissipation factor (DDF, tan δ) and complex capacitance, which can be done in different ways, e.g., using the Extended Debye equivalent circuit model as in [2], Hamon approximation which is uncomplicated to be used.

II. PDC MEASUREMENT

PDC measurements on the stator winding insulation of generators were performed on both phase-to-ground insulation and phase-to-phase (or interphase) insulation. Theoretically, the principle of PDC measurement is when applying a step DC voltage across the interested insulation system, while the current flowing through the insulation was measured using an appropriate ampere meter, which is able to measure the current down to the picoampere range. The current measured in which a step DC voltage (U) was applied is the so-called polarization current (or so-called charge current, relaxation current). Thereafter, when the voltage source was then removed and the insulation under test was short-circuited. The current measured in this process is the so-called depolarization current (or discharge current). The polarization current ($i_p(t)$) can be expressed in (1)

$$i_p(t) = C_0 U\left(\delta(t) + f(t) + \frac{\sigma_0}{\varepsilon_0}\right) \quad (1)$$

where C_0 is the vacuum capacitance, $\delta(t)$ is the delta function, $f(t)$ is the dielectric response function of material, σ_0 is the DC conductivity of the material and ε_0 is the permittivity of free space or vacuum (8.85419×10^{-12} [As/Vm])

The polarization current is comprised of three terms. First, a capacitive current term which occur in the short time that decay with time constant, depend on the series resistance of test circuit and the capacitance of test object. Second, the polarization or absorption current term is caused by the polarization process from dipolar and interfacial polarization. This current decay to nearly zero for long time. Third, the conduction or leakage current term occurs when the voltage source is applied to the insulation. Furthermore, after the step DC voltage source was removed and then the insulation was short-circuited. Since the voltage was absent, so the conduction process was then not appeared in the depolarization current. The current measured in this process is depolarization current ($i_d(t)$), which can be expressed in (2)

$$i_d(t) = -C_0 U\left[\delta(t) + f(t) - f(t+T_c)\right] \tag{2}$$

where T_c is charging time

Furthermore, such dielectric response in the time-domain can be converted into the DDF in the frequency domain to assess the insulation condition [2]. The DDF can be calculated from (3)

$$\tan\delta(\omega) = \frac{\dfrac{1}{\omega R_{dc}} + \sum_{i=1}^{n} \dfrac{\omega R_i C_i^2}{1+(\omega R_i C_i)^2}}{C_{geo} + \sum_{i=1}^{n} \dfrac{C_i}{1+(\omega R_i C_i)^2}} \tag{3}$$

where C_{geo} is the high frequency capacitance or geometric capacitance, R_{dc} is the DC resistance, R_i and C_i is the series resistance and capacitance, representing dielectric loss due to the slow process of polarization phenomena.

Unless the geometric capacitance can be measured from the PDC analyzer, the other parameters above were obtained from fitting the polarization and depolarization current using (4) below

$$i_p(t) = \frac{U}{R_{dc}} + \sum_{i=1}^{n}\left(\frac{U}{R_i}\cdot e^{-\frac{t}{R_i C_i}}\right) \tag{4}$$

$$i_d(t) = \sum_{i=1}^{n} A_i \cdot e^{-\frac{t}{R_i C_i}}$$

where $$A_i = \frac{U}{R_i}\cdot\left(1 - e^{-\frac{T_c}{R_i C_i}}\right)$$

III. Experiment

In the experiment, PDC measurements were conducted on the stator winding insulation of two large turbo-generators, which have the same rate of 50.8 MVA, and 11.5 kV in the power plant (Temperature 30-35 °C, 60-70 %RH). Two investigated generators were labeled as generator A and generator B, respectively. Besides, two test circuit configurations for PDC measurement were used, as shown in Fig. 1. Test circuit 1 was performed by applying a step DC voltage to an interesting phase while the other two phases were grounded. The purpose of test circuit 1 is to measure the current flowing through the bulk of the groundwall insulation and also the leakage or surface current over the endwinding region through the stator core. Alternately, test circuit 2 was performed by applying a step DC voltage to an interesting phase and measuring the current at another phase while the remaining phase was grounded. It can be found that the test configuration of test circuit 2 act as three electrodes configuration with a guard electrode. Thus, the current flowing through the remaining phase and stator core are guarded. The purpose of test circuit 1 is to measure the current flowing through the interphase insulation.

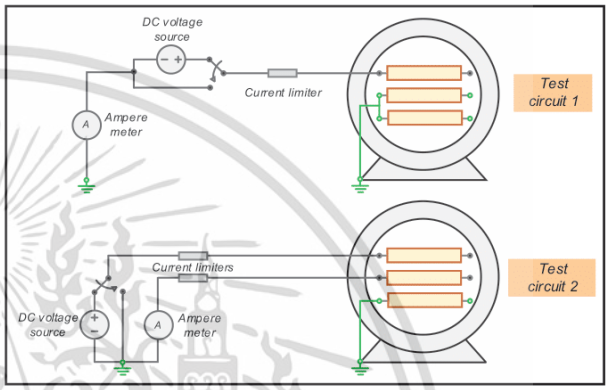

Figure 1. Test circuits for PDC measurement.

Before performing the PDC measurement, the insulation to be tested should be discharged with the appropriate circuit as long as the residue charge is low. Then, the measurement on test circuit 1 was conducted by applying a step DC voltage of 100 V_{dc} while circuit 2 was 200 and 500 V_{dc} for generator B and generator A, respectively. Additionally, the charging time (polarization time, T_c) and discharging time (depolarization time, T_d) for the test circuit 1, are 1100 s, whereas the test circuit 2 is 650 s for both charging and discharging time.

IV. Results

The PDC results of test circuit 1 of the two investigated generators were normalized by dividing the currents with the capacitance of the stator winding insulation to allow the comparison in between, as shown in Fig. 2. The capacitance of the phase-to-ground insulation of the stator winding of the two investigated generators was about 190 nF. Since the PDC results in each phase were similar, only a single phase (Phase A) of the PDC results of test circuit 1 was selected to compare the PDC characteristics of identical rated machines.

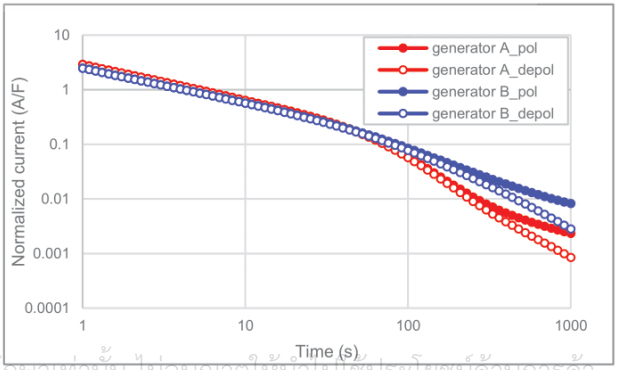

Figure 2. Normalized PDC measured from test circuit 1.

The polarization and depolarization current curves of two generators measuring from test circuit 1 represent the “hump” in the time between 10-100 s, i.e., relaxation peak in the loss factor curve in the frequency domain between 1-10 mHz. Since the hump shape was observed in the polarization current curve, the high value of PI was given. The PI values of generator A and generator B were 34 and 11, respectively. Such a high value of PI was strongly influenced by the stress grading control of the stator winding insulation system [5-6]. Considering the polarization current curve, the current between the time of 100-1000 s shows a “bending curve”, accordingly, resulting in a lower current and a higher IR at the time of 600 s. Besides, the hump curve on the polarization and depolarization current can be seen in literatures [5, 7]. This hump was caused by the influence of the stress grading control system having non-linearity characteristics [5]. In [5-6], it was found that when increasing the test voltage, this hump can be shifted to a lower time. Thus, the influence of the stress grading control on the polarization curve and depolarization curve can be less influenced. However, in this experiment, the low test voltages were employed, so the polarization and depolarization could be affected by such stress grading control. Considering the polarization current measured from test circuit 1, it was found that the contribution of the conduction current of generator A is significantly lower than that of generator B.

The PDC results of test circuit 2 of the two investigated generators are illustrated in Fig. 3. The capacitance of the interphase insulation of the stator winding of the two investigated generators was about 1 nF. As the same for phase-to-ground insulation, since the PDC results in each dual phase were similar, only a single dual phase (Phase A and B) of the PDC results of test circuit 2 was introduced.

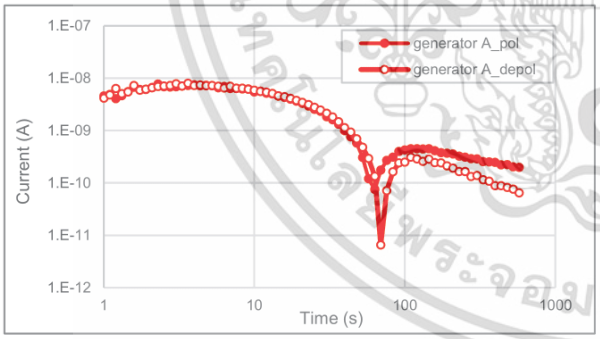

(a)

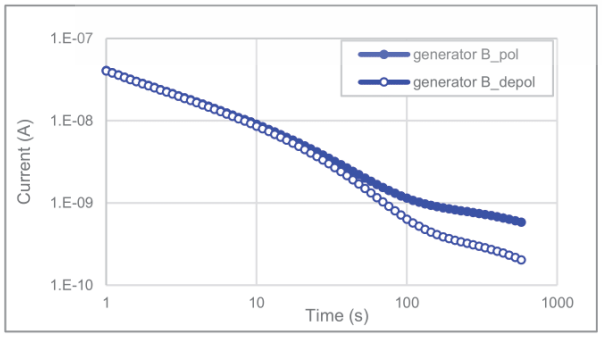

(b)

Figure 3. PDC measured from test circuit 2 of (a) generator A and (b) generator B

From the polarization and depolarization current curves of generator A measuring from test circuit 2, as shown in Fig. 3, it represents the polarity reversal (or Anomalous current) of both polarization and depolarization current at the time of about 60-70 s. Such polarity reversal also causes the reverse of the DDF in the frequency domain. Reference [8] reported that when performing the power factor test on the interphase insulation of the stator winding insulation of generator using the test circuit configuration similar to test circuit 2 for measuring interphase insulation in this experiment, it is possible to obtain the negative value of power factor (also DDF). It causes when the power factor of the interphase insulation is a lower influence when compared with that of phase-to-ground insulation [8]. Accordingly, the DDF of generator A, illustrated in Fig. 4, was relatively low (compared with the DDF of generator B), so it can be implied that the power factor (or DDF in this case) was lower when compared with that of phase-to-ground insulation. However, the test circuit for measuring the PI and IR (also PDC measurement) of interphase insulation in IEC 60034-27-4 used a float test instrument to measure [9]. From such a circuit configuration, the guard electrode is not needed.

In the case of generator B, polarization and depolarization current curves revealed the hump shape as seen in the polarization and depolarization curve of phase-to-ground insulation. Besides, both polarization and depolarization current were not reversed. The results exhibit more significance on the dielectric loss of the interphase insulation than that of the phase-to-ground insulation.

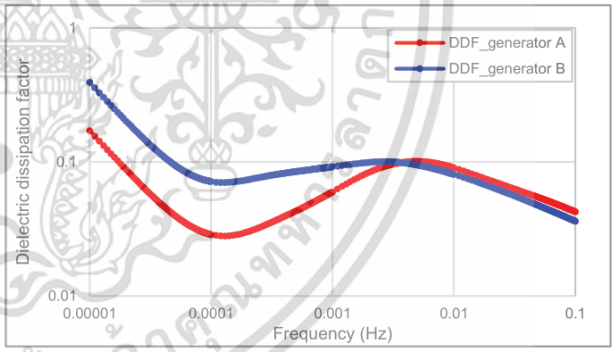

Figure 4. DDF of phase-to-ground insulation of two investigated generators.

From the DDF of phase-to-ground insulation of two investigated generators calculated using (4) as shown in Fig. 4, it was found that the relaxation peak occurs in the frequency range of 1-10 mHz. However, the relaxation peak of the generator A, slightly occurs in a higher frequency than that of generator B. Since a slight shift toward the high frequency of generator A than generator B. The shifting of the relaxation peak toward high frequency can be implied by the aging of the stator winding insulation [10]. Although the relaxation peak has occurred in a higher in the case of generator A. However, a slight shift was not significant. Besides, when considering the lower frequency range, the straight line in the lower frequency range, i.e., below 0.1 mHz (in this case), represents the contribution of conduction loss in the DDF curve. The conduction loss in DDF of generator A was lower than that of generator B, which is in good agreement with the lower contribution of the conduction current in the polarization current in the time domain.

V. Conclusion

In this paper, PDC measurements were conducted on two generators to compare the PDC characteristics of identical-rated machines. In the case of phase-to-ground insulation, the effect of the stress grading control system can strongly influence both polarization and depolarization currents resulting in the hump shape and significantly high PI value, which is calculated from the polarization current. In the case of generator A, the contribution of the conduction current in the polarization current was low, resulting in the low conduction loss in the DDF in the lower frequency range. Besides, in the case of the interphase insulation, the polarity reversal of the polarization and depolarization current was due to the dielectric loss of the interphase insulation is a lower influence when compared with that of phase-to-ground insulation. Therefore, the PDC measurement combined with the parameters in the frequency domain can be a valuable tool for assessing the condition of the stator winding insulation of the generator.

Acknowledgment

The authors thank all staff in Dielectric Analytika laboratory (Dika Lab), King Mongkut's Institute of Technology Ladkrabang, for helping in the PDC measurement.

References

[1] G. C. Stone, E. A. Boulter, I. Culbert, and H. Dhirani, "Electrical Insulation for Rotating Machines," 1st Ed., Wiley-IEEE Press, 2004.

[2] W. S. Zaengl, "Dielectric spectroscopy in time and frequency domain for HV power equipment. I. Theoretical considerations," in IEEE Electrical Insulation Magazine, vol. 19, no. 5, pp. 5-19, Sept.-Oct. 2003.

[3] G. R. Soltani and E. David, "Condition assessment of rotating machine winding insulation by analysis of charging and discharging currents," Conference Record of the 2006 IEEE International Symposium on Electrical Insulation, pp. 336-339, 2006.

[4] S. A. Bhumiwat, "Insulation resistance and polarization of rotating machines," 2011 Electrical Insulation Conference (EIC, pp. 249-253), 2011.

[5] E. David, R. Soltani and L. Lamarre, "PDC measurements to assess machine insulation," in IEEE Transactions on Dielectrics and Electrical Insulation, vol. 17, no. 5, pp. 1461-1469, October 2010.

[6] IEEE Std 43-2013 (Revision of IEEE Std 43-2000), "Recommended Practice for Testing Insulation Resistance of Electric Machinery".

[7] S. A. Bhumiwat, "Depolarization index for dielectric aging indicator of rotating machines," in IEEE Transactions on Dielectrics and Electrical Insulation, vol. 22, no. 6, pp. 3126-3132, December 2015.

[8] L. Pong, "Review Negative Power Factor Test Results and Case Study Analysis," The 2002 Int. Conf. of Doble Clients; Boston/ USA, 2002.

[9] IEC 60034-27-4:2018, "Rotating electrical machines - Part 27-4: Measurement of insulation resistance and polarization index of winding insulation of rotating electrical machines".

[10] E. David and L. Lamarre, "Low-frequency dielectric response of epoxy-mica insulated generator bars during multi-stress aging," in IEEE Transactions on Dielectrics and Electrical Insulation, vol. 14, no. 1, pp. 212-226, Feb. 2007.

Biography

Personal Data:

Name:	B. Eng. Siwakorn Jeenmuang
Date of Birth	Oct 15th, 1998
Place of Birth	Pattani
Nationality	Thai
Email	siwakorn.je@gmail.com
Telephone	+66-96-794-5233

Education:

August 2017 to June 2021	B. Eng. in Electrical Engineering (First Class Honors) King Mongkut's Institute of Technology Ladkrabang (KMITL), Bangkok, Thailand

Research Interest:

- High-voltage Measurement Techniques
- High-voltage Equipment Monitoring and Diagnosis
- Insulating Systems of High Voltage Rotating Machines, Power Transformers and Underground Cables, Testing and Diagnosis

Industrial Projects:

- Condition Assessment of Stator Winding Insulation of Generator (2021-2023)
- Condition Assessment of Stator Winding Insulation of High Voltage Motor (2021-2023)
- Root Cause Analysis of the Cable Termination Explosion (2021)
- 22 kV Underground Cable Assessment (2022)
- 115 kV Underground Cable Assessment (2022)
- Off-line Partial Discharge Measurement of 11 kV Generator Stator Coils (2022)
- Water Tree Examination of 6.6 kV Cable Terminations (2023)
- Root Cause Analysis of the 115 kV Dry Type Plug-in GIS Cable Termination Explosion (2023)

List of Publications (2021-2023):

First-Author Conference Publication

1. S. Jeenmuang, P. Pannil, S. Mongkolsatitpong, S. Trakuldit, V. Wuti and N. Pattanadech, "The Application of Polarization and Depolarization Current on the Large Turbo-generators," 2022 9th International Conference on Condition Monitoring and Diagnosis (CMD), Kitakyushu, Japan, 2022, pp. 118-121, doi: 10.23919/CMD54214.2022.9991272.

Co-Author Conference Publications

1. W. Rojanasunan, P. Chancharoensook, S. Jeenmuang, S. Mongkolsatitpong, N. Pattanadech and D. Suksawat, "The Effects of Coupling and Grounding on the Partial Discharge Pulse Propagation in the Underground Cable," 2022 9th International Conference on Condition Monitoring and Diagnosis (CMD), Kitakyushu, Japan, 2022, pp. 87-91, doi: 10.23919/CMD54214.2022.9991722.

2. N. Tongchim, N. Phansiri, S. Jeenmuang and N. Pattanadech, "Design of a Multi-channel PD Detector for Improving Common-mode Noise Reduction Performance in Measuring and Monitoring System," 2022 9th International Conference on Condition Monitoring and Diagnosis (CMD), Kitakyushu, Japan, 2022, pp. 583-587, doi: 10.23919/CMD54214.2022.9991533.

Co-Author Journal Publications

1. Norasage Pattanadech, Natnaree Phumipunepon, Chissanupong Srinangyam, Siwakorn Jeenmuang and Chanin Bunlaksananusorn, “Dielectric analysis of degraded stator bars of a hydro generator,” Energy Reports, vol. 8, April 2022, pp. 313-321, doi: https://doi.org/10.1016/j.egyr.2021.11.143.

2. Norasage Pattanadech, Natthawut Phloymuk, Pethai Nimsanong, Chissanupong Srinangyam, Siwakorn Jeenmuang and Chanin Bunlaksananusorn, “Additional parameters for elucidation of the dielectric behavior of stator winding in high voltage motors,” Energy Reports, vol. 8, November 2022, pp. 3629-3635, doi: https://doi.org/10.1016/j.egyr.2022.02.282.

3. Yannaphol Kittikhuntharadol, Norasage Pattanadech, Sakda Maneerot, Korraya Jongvilaikasem, Kittipod Jariyanurat, Siwakorn Jeenmuang, Patt Udomluksananon, Komin Chumpiboon, Chanin Bunlaksananusorn, “Physical and chemical properties’ comparison of natural ester and palm oil used in a distribution transformer,” Energy Reports, Vol. 9, March 2023, Pages 549-556, https://doi.org/10.1016/j.egyr.2022.11.100.